



저작자표시-비영리-변경금지 2.0 대한민국

이용자는 아래의 조건을 따르는 경우에 한하여 자유롭게

- 이 저작물을 복제, 배포, 전송, 전시, 공연 및 방송할 수 있습니다.

다음과 같은 조건을 따라야 합니다:



저작자표시. 귀하는 원저작자를 표시하여야 합니다.



비영리. 귀하는 이 저작물을 영리 목적으로 이용할 수 없습니다.



변경금지. 귀하는 이 저작물을 개작, 변형 또는 가공할 수 없습니다.

- 귀하는, 이 저작물의 재이용이나 배포의 경우, 이 저작물에 적용된 이용허락조건을 명확하게 나타내어야 합니다.
- 저작권자로부터 별도의 허가를 받으면 이러한 조건들은 적용되지 않습니다.

저작권법에 따른 이용자의 권리는 위의 내용에 의하여 영향을 받지 않습니다.

이것은 [이용허락규약\(Legal Code\)](#)을 이해하기 쉽게 요약한 것입니다.

[Disclaimer](#)

박사학위논문

Baicalein suppresses stem cell-like characteristics of resistant human breast cancer cells MDA-MB-231 by up-regulation of interferon-induced protein with tetratricopeptide repeats 2

제주대학교 대학원

차세대융복합과학기술협동과정

고 소 예

2019년 8월

Baicalein suppresses stem cell-like characteristics of resistant human breast cancer cells MDA-MB-231 by up-regulation of interferon-induced protein with tetratricopeptide repeats 2

지도교수 김소미

고 소 예

이 논문을 이학 박사학위 논문으로 제출함

2019 년 8 월

고소예의 이학 박사학위 논문을 인준함

심사위원장

이 등 선

위 원

김 소 미

위 원

조 문 제

위 원

최 학 선

위 원

문 정 용

제주대학교 대학원

2019 년 8 월



Baicalein suppresses stem cell-like characteristics of resistant human breast cancer cells MDA-MB-231 by up-regulation of interferon-induced protein with tetratricopeptide repeats 2

So Yae Koh

(Supervised by Professor Somi Kim Cho)

A thesis submitted in partial fulfillment of the requirement for the degree of Doctor of Science

2019. 8.

The thesis has been examined and approved.

DangSun Lee

Somi Kim Cho

Jeong Cho

Hack Sun Choi

Jeong Yong Moon

June 5th, 2019

Department of Advanced Convergence Technology & Science

Graduate School

Jeju National University



CONTENTS

1. Abstract.....	1
2. Introduction.....	2
2.1. Breast cancer	
2.2. Cancer stem cells	
2.3. Epithelial to mesenchymal transition	
2.4. Invasion and metastasis	
2.5. Phytochemicals	
2.6. Baicalein	
2.7. Interferon-induced proteins with tetratricopeptide repeat 2	
2.8. Transcriptomic analysis	
2.9. Summary	
3. Materials and methods.....	9
3.1. Reagents	
3.2. Cell culture and resistant cell generation	
3.3. Cell viability	
3.4. Cell morphology	
3.5. Clonogenic assay	
3.6. Mammosphere	
3.7. RNA extraction, cDNA synthesis, and Realtime PCR	
3.8. Wound healing assay	
3.9. Invasion assay	
3.10. Flow cytometry	
3.11. Western blot	
3.12. Transcriptomic analysis	

- 3.13. Pathway analysis
- 3.14. Gene expression analysis
- 3.15. Statistical analyses

4. Results..... 16

- 4.1. MDA-MB-231/IR cells developed radio-resistance
- 4.2. MDA-MB-231/IR cells developed chemo-resistance
- 4.3. Chemo- resistance of MDA-MB-231/IR cells evaluated by Annexin V/PI assay
- 4.4. MDA-MB-231/IR cells exhibited epithelial to mesenchymal morphology compared to parental cells
- 4.5. MDA-MB-231/IR cells exhibited enhanced migration and invasion ability compared to parental cells
- 4.6. Mammosphere forming ability and expression levels of stem cell-like markers were enhanced in MDA-MB-231/IR cells than those of parental cells
- 4.7. MDA-MB-231/IR cells exhibited stem cell-like characters compared to its parental cells
- 4.8. Transcriptomics analysis on MDA-MB-231/IR cells
- 4.9. Cancer resistance was reported in 12 DEGs of MDA-MB-231/IR
- 4.10. Baicalein effectively targeted chemo- and radio-resistance MDA-MB-231/IR cells
- 4.11. Baicalein reversed expression of IFIT2 in MDA-MB-231/IR
- 4.12. Baicalein reduced protein expression level of Slug
- 4.13. Baicalein inhibited EMT capacity of MDA-MB-231/IR
- 4.14. Baicalein diminished the mammosphere formation and expression of marker proteins in MDA-MB-231/IR
- 4.15. Baicalein diminished the stem cell-like characters of MDA-MB-231/IR
- 4.16. Baicalein increased expression levels of apoptosis-related proteins on MDA-MB-231/IR
- 4.17. Baicalein induces apoptosis on MDA-MB-231/IR cells
- 4.18. Baicalein co-treatment reversed radio- resistance in MDA-MB-231/IR
- 4.19. Baicalein co-treatment reversed chemo- resistance in MDA-MB-231/IR
- 4.20. The expression of IFIT2 affects survival in patients

5. Discussion.....	59
6. References.....	70

1. Abstract

Breast cancer is the second leading cause of cancer death for woman and the most prevalent type of cancer. Triple negative breast cancer (TNBC) is the most poor prognosis subtype of breast cancer and represented with high tumor grade and metastasis. We generated radio- and chemo- resistance cells by irradiation (IR), MDA-MB-231/IR. The resistance cells were enhanced in migration (1.72-fold), invasion (1.48-fold), and stem cell-like characteristics such as mammosphere formation (1.44-fold) and side population (1.67-fold). Pathway analysis exhibited that MDA-MB-231/IR had activated including NF- κ B pathway (11%), TNF signaling pathway (10%), and Toll-like receptor pathway (10%). Within 77 differentially expressed genes (DEGs) demonstrated by our transcriptome analysis, 12 DEGs were associated with cancer resistance on MDA-MB-231/IR; the genes were AKR1C1 (6.83log₂ fold), FTL (6.64-log₂ fold), MK (2.92-log₂ fold), LG3BP (6.01-log₂ fold), GFPT2 (3.04-log₂ fold), TGFBI (3.34-log₂ fold), AKR1C3 (3.87-log₂ fold), CCDC69 (2.96-log₂ fold), AKR1C2 (3.87-log₂ fold), TWF1, PKP3, and IFIT2 (-2.84-log₂ fold). Baicalein induced apoptosis on MDA-MB-231/IR and the half maximum inhibitory concentration (IC₅₀) of baicalein was $39.58 \pm 2.86 \mu\text{M}$. Baicalein reversed radio- and chemo- resistance, migration (0.61-fold), invasion (0.43-fold), mammosphere formation (0.12-fold), and expression of CD44^{high} and CD24^{low} population of MDA-MB-231/IR (0.48-fold) while increasing the expression of interferon-induced protein with tetratricopeptide repeats 2 (IFIT2) (3-fold in mRNA and 27-fold in protein level). Using the cancer genome atlas (TCGA) database, IFIT2 expression was concerned with metastasis and poor prognosis marker for TNBC patients.

2. Introduction

2.1. Breast cancer

Breast cancer is the most prevalent type of cancer and the second leading cause of cancer death for women worldwide. Also it is expected to account for 29% of all new cancer diagnoses (Siegel et al., 2016). Breast cancer has been divided into subtypes differentiated by the expression of receptors: HR-positive (luminal), HER2-amplification, and TNBC (triple negative breast cancer). Hormone receptor (HR)- positive cancer is the most common subtype of breast cancer, in which approximately 70% of breast cancer patients are diagnosed. The HR-positive cancer can be classified to three subtypes in detail: 1)ER/PR-positive/ HER2-negative/ Ki67-negative, 2)ER/PR-positive/ HER2-negative/ Ki67- positive, 3)ER/PR-positive/ HER2-positive/ Ki67-positive. The HR is a receptor expressed in the nucleus and when HR is activated by estrogen PI3K/Akt pathway and MAP kinase pathways are followed (Levin et al., 2008).

While only 15-20% of breast cancer patients are classified to triple-negative breast cancer (TNBC) which is lack of ER, PR and HER2 over-expression, however the TNBC patients represents poor prognosis with unfavorable features in histologic grades, tumor sizes, and metastasis (Haffty et al., 2006; Dent et al., 2007). It is a challenge to the TNBC patients which hormone therapy or receptor targeting drugs are not responding to them in despite of advances in chemical or hormonal therapies. Moreover, heterogeneity of TNBC indicates the higher probability survival from chemotherapy. The heterogenous character of TNBC leads to application of novel agents that are targeting specific molecules or circumventing innate resistant to chemotherapy which could provide a protective effect against radiation (Oakman et al., 2010; Bianchini et al., 2016; Luzhna et al., 2015).

2.2. Cancer stem cells (CSCs)

Cancer stem cells also called tumor initiating cells (TICs), are a particular subpopulation of cells in cancers, including breast cancer, that are capable of self-renew and differentiate into the heterogeneous lineages of cancer cells that compose the tumor (Lapidot et al., 1994). CSCs are illustrated to be positioned at the top of the tumor hierarchy and considered to develop therapeutic resistance, recurrence and metastasis (Zhou et al., 2009; Meacham et al., 2013). TNBC subtype is reported to contain higher CSCs which represented as therapy resistance. There are several ways to identify CSCs from cancer cells but the expression of cell surface markers and some membrane transporters are used for identification (Schatton et al., 2009; Dean et al., 2005). It has been reported that the cells with expressions of CD44, CD24, and CD133 on their surfaces are considered to breast CSCs (Al-Hajj et al., 2003; Liu et al., 2013). Furthermore, embryonic regulators, like Oct4 and Twist, and cell membrane adenosine triphosphate-binding cassette transporters, for example, MRP1, ABCG2, and MDR1, are overexpressed in the CSCs of breast cancer (Scharenberg et al., 2002). Side population assays are one of the well-known techniques to detect CSCs by effusion activity of ABC transporters with Hoechst 33342 (Scharenberg et al., 2002).

2.3. Epithelial to mesenchymal transition (EMT)

Epithelial to mesenchymal transition is a fundamental process of development of embryo but a crucial event for malignancy in cancer. Mutations in Wnt, Notch and Hedgehog pathways are considered deviate normal stem cell from regulation signals (Beachy et al., 2004). The progression of EMT process is correlated with aggressive cancer development and tumor malignancy (Thiery, 2003). Moreover, CSCs present this morphological change

that includes the loss of cell-cell adhesion and acquisition of migration and invasion abilities (Hemavathy et al., 2000; Blanco et al., 2002). In adherens junctions, membranous E-cadherin is a hallmark of EMT and gene repressors such as Slug, Snail, or ZEB1/2, transcriptionally regulates its expression (Conacci-Sorrell, M. et al. 2003).

2.4. Invasion and metastasis

Invasion and metastasis are characteristics of CSCs that those cells are penetrating extra-cellular matrix (ECM), basement membranes, and endothelial walls to migrate and colonize distant organs (Fidler, 2003). The invasion events include the changes in cell-cell adhesion, cell-ECM adhesion, protease activities, and chemo-sensing receptors (Friedl, 2011). These incidents are considered to detriment by causing dissemination of tumor and cancer progression (Jang et al., 2015). Twenty to fifty percent of primary breast cancer patients would end up with metastatic disease although only up to 6 % of the breast cancer patients were initially diagnosed to have metastasis (Lu et al., 2009). Therefore it is urgent to seek therapies that could target both migration and invasion in breast cancer.

2.5. Phytochemicals

Plants have been used for medicinal or clinical substances from ancients and anti-cancer drugs created in modern times were also based on structures of natural chemicals (Cragg et al., 2013): more than 50% of novel anti-cancer drugs were obtained or based on chemical structures from natural sources, especially herbs (Amin et al., 2009). The importance of plant derived chemicals lies here. On top of that, researchers have found and highlighted the

importance of understanding the biological characteristics of active compounds of herbal remedies such as polyphenols, not only because of their effect but also economical accessibility (Nowak et al., 2013; Bahmani et al., 2016). Phenolic compounds are a kind of secondary metabolites of plants which is abundantly distributed (Mocanu et al., 2015). The phenolic compounds have more than one of aromatic ring with one or more hydroxyl groups and are expected to have anti-cancer activities (Crozier et al., 2009).

Flavonoids are one of the widely found substances from plants like fruits and vegetables, and they are widely investigated for efficacy of human health. The skeleton of flavonoids consist a C6-C3-C6 ring (also described as A-C-B ring), which is called benzopyran, and the locations of hydroxyl groups in different rings determine subclasses of flavonoid (Choi et al., 2012; Kanadaswami et al., 2005; Oracz et al., 2015).

Flavone is one the flavonoid with ketone group on C3 ring (C ring) in the basal structure and most well-known natural flavones include luteolin, apigenin, and baicalein for their activities on anti-oxidant, anti-cancer, anti-proliferative and kinase inhibiting effects (Kanadaswami et al., 2005). The influence of flavones on cancer was reported that they could interfere progressive phenomena of cancer (Ravishankar et al., 2013). Flavonols have a hydroxyl group on the 3-position of the C3 ring and previous studies have concluded that the intake of flavonols along with flavones decreased a risk breast cancer (Hui et al., 2013). Quercetin, kaempferol, myricetin, and rutin are the main representatives of flavonols and they are reported to have a role in preventing carcinogenesis (Choi et al., 2018; Kim et al., 2008, Iriti et al., 2017).

2.6. Baicalein

Baicalein is one of active compound of the roots of *Scutellaria baicalensis* Georgi which is a traditional herb in East Asia (Kim et al., 2001). The phytochemical is demonstrated for its biological benefits on reducing tumor progression, inflammation, fibrosis and also on targeting the tumor microenvironment (Bie et al., 2017; Wang et al., 2015; Wu et al., 2011). Only few studies demonstrated the anti-cancer effects of baicalein in TNBC and most of them were focused in suppression of migration and invasion. Baicalein can target TNBC cells by increasing ER stress or lowering mitochondrial membrane potential through induction of intra-cellular reactive oxygen species (ROS) in caspase dependent pathway (Lee et al., 2008) or by down-regulating SATB1 and Wnt/ β -catenin pathway (Ma et al., 2016). However, the effect of baicalein on therapy resistance TNBC cells was still not studied.

2.7. Interferon-induced proteins with tetratricopeptide repeat 2 (IFIT2)

IFIT2 is a protein of 54 kDa (472 amino acids) and it is one of the members of IFITs in human. The family is induced by interferons or through Toll-like receptors, RIG-1-like receptors. They are considered to play a role in immune response by recognizing structures of viral RNA and inhibiting mRNA translation (Pichlmair et al., 2011; Zhou et al., 2013). Expression of IFIT2 is negatively co-expressed by Wnt/ β -catenin signaling and in colorectal cancer cells (Ohsugi et al., 2017), and IFIT2 especially induces apoptosis in cervical cancer cells via mitochondria pathway (Stawowczyk et al., 2011). Few researchers have focused on the correlation of IFIT2 and prognosis in patients in oral cancer and gastric cancer (Lai et al., 2008; Chen et al., 2018), but studies regarding their roles in breast cancer have been limited.

2.8. Transcriptomic analysis

Transcriptomics analysis is the large-scaled study using the high-throughput techniques to examine RNA molecules of cells (Velculescu et al., 1997; Carninci et al., 2005; Cieslik et al., 2017). Unlike DNA, the transcribed RNA gives information of cells including cell types, regulation mechanisms, and morphological features (Hughes et al., 2000). These days, transcriptomics is often applied to identify biological processes of cancer for novel clinical application. Cancer cells are distinguished from normal cells by altered gene expression and protein function, so that understanding transcriptome of cancer cells gives better information underlying mechanisms such as resistance and pathogenesis (Chang et al., 2003; Staunton et al., 2001). The development of sequencing techniques like next-generation sequencing (NGS) methodology and shotgun sequencing enabled researchers to apply transcriptomic analysis on their works and to store the results of microarray and RNA-seq to database, for example, The Cancer Genome Atlas (TCGA), the Human Protein Atlas, the Encyclopedia of DNA Elements (ENCODE), and the Cancer Cell Line Encyclopedia (CCLE). With those databases, researchers can approach to elucidate the structure of global gene expression by bioinformatics and computational biology.

2.9. Summary

In this paper, we focused in the effects of baicalein on therapy resistance TNBC cells which were generated by irradiation. Comparing normal TNBC cells with resistant counterparts, chemo- and radio-resistant TNBC cells increased migrating and invasive ability as well as stem cell-like character phenomena. Baicalein was the most effective phytochemical among we tested. Transcriptome analysis revealed 12 genes that were

reported with cancer resistance, and one of the genes, IFIT2 was found to reverse its transcriptional expression after baicalein treatment. Kaplan-Meier plot of TNBC patients indicated that poor prognosis was related to low IFIT2 expression.

3. Materials and Methods

3.1. Reagents

DMEM medium, trypsin/EDTA, TRIzol, FBS, BSA, bFGF, insulin, EGF, B-27 supplement were purchased from Invitrogen Inc. (Carlsbad, CA, USA). Baicalein, myricetin, luteolin, kaempferol, quercetin, rutin, HEPES, adriamycin (doxorubicin), RNase A, Hoechst 33342 dye, propidium iodide (PI), 2',7'-dichlorofluorescein diacetate (H₂DCF-DA) were obtained from Sigma chemical Co. (St. Louis, MO, USA). Matrigel matrix, Mitoscreen (JC-1) kit and Annexin V-FITC Apoptosis detection kit were obtained from BD Bioscience (Franklin Lakes, NJ, USA). From Santa Cruz Biotechnology (Dallas, TX, USA), cisplatin was purchased. Dimethyl sulfoxide (DMSO) and 3-(4,5-Dimethylthiazol-2-yl)-2,5-diphenyl-tetrazolium bromide (MTT) were purchased from Amresco (Solon, OH, USA). PVDF membrane was purchased from Pierce Protein Biology (Rockford, IL, USA) and BCA protein assay kit was obtained from Millipore Ltd. (Billerica, MA, USA). Phosphate buffered saline (PBS) and BS ECL Plus kit were obtained from Biosesang (Gyeonggi, Korea).

3.2. Cell culture and resistant cell generation

MDA-MB-231 and its derived cells were cultured in DMEM medium supplemented with 10% of FBS and 1% of antibiotics, and incubated at 37 °C in a humidified incubator with 5% of CO₂. After subculture, when the cell's confluency arrived at 70-80%, irradiation of 2 Gy was performed. The irradiation was performed using a ⁶⁰CO Theatron-780 teletherapy unit (dose rate: 1.52 Gy/min) at Applied Radiological Science Institute in Jeju National University. Two gray of radiation was irradiated once a day, 5 days in a row, for 5

weeks. Subculture to new dish was done after 5 times of irradiation and medium was changed to new medium twice a week. Twenty-five times of irradiations were performed in 5 weeks and the radiated cells were cultured for a month before starting following assays.

3.3. Cell viability

The cell viability was determined by MTT assay after sample treatment. Using the conversion MTT to formazan crystals by mitochondrial dehydrogenases, the percentage of live cells can be calculated. Briefly, cells plated in 96-well plates at a density of 1×10^4 cells/mL were treated with indicated samples diluted in DMEM medium with various concentrations. When radiation was treated, 1×10^4 of cells were directly radiated and seeded for 4 extra days. After that, the medium was suctioned and 100 μ L of MTT solution (solved in distilled water, final concentration of 1 mg/mL) was added. After 3-4 h of incubation, the media were aspirated and the formazan was dissolved in DMSO (150 μ L). Absorbance (at 570 nm) was detected by Tecan microplate reader (Salzbrug, Austria).

3.4. Cell morphology

Cell morphology was observed under an Olympus light or fluorescence microscope (Essex, UK). Cells were checked before subculture under the light to check confluency of dishes. Cell's morphology was envisaged under the light microscope and captured by program.

3.5. Clonogenic assay

To calculate the surviving fraction after radiation, colony forming assay was carried out. 1×10^4 of cells was prepared by counting after trypsinization and irradiation were conducted. Irradiation was performed with 0, 2, 4, 6, 8 Gy of γ -ray. After radiation, cells were directly seeded on 12-well plate for 5 days. Colonies were washed and fixed by cold methanol for 10 min. The methanol was aspirated and crystal violet was used for dyeing. Colonies were counted by software program NIST's integrated colony enumerator (NICE; Choi et al., 2018; <ftp://ftp.nist.gov/pub/physics/mlclarke/NICE>).

3.6. Mammosphere

To form mammosphere, DMEM was supplemented with 1 μ M insulin, 1% of BSA, 20 ng/mL EGF, 10 ng/mL bFGF and B-27 supplement. Cells were washed before seeded at a density of 2×10^2 in non-coating 24-well plate with the described media. After incubation for a week, mammospheres comprised of at least 50 cells were counted.

3.7. RNA extraction, cDNA synthesis, and Realtime PCR

Cells were prepared for 24 h before RNA extraction following to manufacturer's protocol. cDNA was synthesized using Promega reverse transcription kit (Madison, WI, USA), using 1 μ g of RNA. To confirm the quality of cDNA synthesis, glyceraldehyde 3-phosphate dehydrogenase (GAPDH) was used as a control. Quantitative realtime PCR was

initiated by incubating at 95 °C for 15 min and 40-50 cycles of denaturation, annealing and elongation steps were set. The relative levels of gene expression were calculated by the following method.

The relative level of gene expression = $2^{-\Delta\Delta Ct}$; Ct is cycle threshold.

$\Delta Ct = Ct_{\text{gene}} - Ct_{\text{reference}}$; reference is GAPDH.

$\Delta\Delta Ct = (\Delta Ct_{\text{gene}} \text{ of MDA-MB-231/IR}) - (\Delta Ct_{\text{gene}} \text{ of MDA-MB-231})$

3.8. Wound healing assay

Cells were counted at 1×10^5 cells per well and incubated to be confluent on the 6-well plate for 24 h in mono-layer. With sterilized 1000- μL tip of pipette, scratch was made in a shape of cross. After the scratching, the plate was washed with PBS and refilled with new media. The width of gap was measured just after scratch (0 h) and 24 h after scratch by image capturing program. The width was measured and the rate of migration was calculated as the following formula.

Wound healing (%) = $\{1 - (\text{width of 24 h after scratch}) / (\text{width of 0 h after scratch})\} \times 100$

3.9. Invasion assay

One hundred μL of 10% Matrigel solution was filled in the upper well of transwell

system before performing assay. Cells were prepared and transferred to the upper well with DMEM media. In the bottom well, 600 μ L of 2% FBS-DMEM media were filled. Using cotton swaps, cells were removed from the insert after 24 h incubation, fixed with fixative (1:1 acetone/methanol) and dyed with crystal violet. The colored invading cells were captured under microscope and the number of cells was counted by Image J and the invasive rate of the cells were compared.

3.10. Flow cytometry

To detect cell cycle, the treated cells were washed and fixed in 70% ethanol. Two hours before analysis, RNase A and PI were diluted in 2 mM EDTA-PBS and treated at 37 °C. The intensities of fluorescence were measured by FACSCalibur (BD Bioscience). The intracellular reactive oxygen species (ROS) levels were measured using 10 μ M of H₂DCF-DA. Cells were prepared and incubated with the dye for 15 min and resuspended for analysis. To detect apoptosis, Annexin V-FITC was utilized following the manufacturer's protocol. Briefly, cells were mixed with Annexin V-FITC and PI for 15 min at room temperature. To detect cell surface markers, CD44-FITC and CD24-PE conjugated dye were incubated with cells for 20 min. Side population was observed using Hoechst 33342. After detaching, cells were diluted with the mix of DMEM buffered with 1 mM HEPES, 5 mM Hoechst 33342 and 2% of FBS for 2 h. The Mitoscreen kit was utilized following to the manufacturer's protocol. JC-1 dye was diluted with cells for 15 min and washed, centrifuged and resuspended in PBS.

3.11. Western blot

Cells were prepared at a density of 1×10^5 on 60 mm plate. Cells were lysed with RIPA buffer supplemented with protease inhibitor cocktail and phenylmethylsulfonyl fluoride and centrifuged for 20 min. Only supernatant was collected and diluted after BCA protein assay. The lysates were separated on 10-12% SDS-PAGE and transferred to PVDF membranes. Primary and secondary antibodies were incubated with the membrane after blocking with 5% of non-fat dried milk in TTBS. Protein bands were detected by BS ECL kit.

3.12. Transcriptomic analysis

Total RNA was extracted using TRIzol and one μg of the RNA was utilized to construct a library using Illumina TruSeq kit (Illumina Inc., San Diego, CA, USA). Poly-T oligo-attached magnetic beads were used for purification. RNA-seq was performed according to the manufacturer's instructions by Macrogen Inc. (Seoul, Korea). Abundance of the transcriptome was determined differentially expressed genes (DEGs) with statistical significance ($P < 0.001$ and at least 2 fold changes) using EdgeR.

3.13. Pathway analysis

We utilized the different modules of the Database for Annotation, Visualization and Integrated Discovery (DAVID, Ver. 6.8) for prediction of pathways and Gene Ontology (GO) associated with MDA-MB-231/IR.

3.14. Gene expression analysis

The cancer genome atlas (TCGA), KM plotter and Xena browser was used for analyze. The relapse free survival of TNBC patients with high or low expression of the gene was detected. The correlation of genes' expression was compared by R program. Gene expressions according to cancer sample types were also analyzed.

3.15. Statistical analyses

Statistical analyses were performed using a one-way analysis of variance and t-test by SPSS (IBM Corp., NY, USA). The p-value less than 0.05 was considered to be significant.

4. Results

4.1. MDA-MB-231/IR cells developed radio-resistance

To gain a better understanding of mechanism of acquired radio- and chemo-resistance in breast cancer, we designed and generated the resistant cancer cells by repetitive 2 Gy irradiations up to total 50 Gy. We named the survived cells MDA-MB-231/IR.

As MDA-MB-231/IR cells had survived from radiation, surviving fraction and cell viability were measured in MDA-MB-231 and its derivative resistant cell MDA-MB-231/IR cells to validate radio-resistance in MDA-MB-231/IR. Cells were exposed to a range of single radiation doses (2–8 Gy) and surviving fraction was calculated using the clonogenic assay. The survival fraction of MDA-MB-231/IR cells was higher than the survival fraction of MDA-MB-231 cells, showing that acquired radio-resistance in MDA-MB-231/IR cells after irradiation. Cell viability assay was also conducted with MTT assay to confirm the radio-resistance of MDA-MB-231/IR after irradiation. The results showed at Figure 1C and we compared the viability with the concept of LD 50 (50 % Lethal dose of gamma ray) which is the estimated dose of radiation expected to kill 50 percent of an exposed population (Hunter N.R., et al, 2013) or IC 50 (Lee H-J., et al., 2013). The LD 50 value of irradiation on MDA-MB-231 cells was 3.48 ± 0.13 Gy, whereas the LD 50 value of irradiation on MDA-MB-231/IR cells was 7.11 ± 0.16 Gy. MDA-MB-231/IR showed much higher surviving ability compared to MDA-MB-231 after irradiation doses we tested.

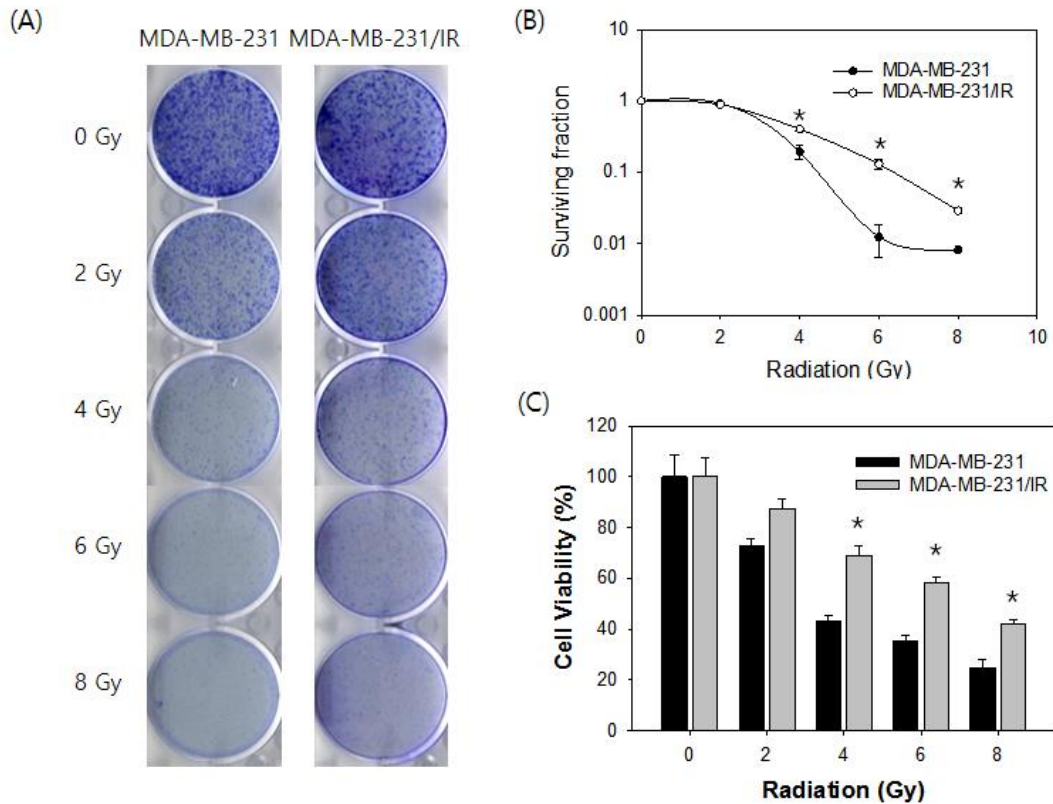


Figure 1. MDA-MB-231/IR developed resistance to irradiation compared to its parental cell, MDA-MB-231. Clonogenic assay of MDA-MB-231 and MDA-MB-231/IR was evaluated 5 days after irradiation of the indicated dose of gray (Gy) (A). Colonies were counted by NIST's integrated colony enumerator (NICE) for surviving fraction (B). MTT assay of MDA-MB-231 and MDA-MB-231/IR was evaluated 4 days after irradiation of indicated doses of gray (C). Values represent means \pm standard deviation (SD) (n= 3) (* p < 0.05).

4.2. MDA-MB-231/IR cells developed chemo-resistance

It is acceptable that one resistant mechanism could be shared with several stimuli, so that we tested if radiation resistant cell MDA-MB-231/IR cells have chemo-resistance. Among many anticancer drugs, adriamycin, paclitaxel, or cisplatin are the most frequently used drugs for breast cancer therapy, especially for metastatic breast cancer. Adriamycin works by intercalating in DNA and inhibiting topoisomerase. Cisplatin is another anti-cancer drug, which has a different mechanism from adriamycin. Cisplatin belongs to the platinum-based drugs and it binds to guanine of DNA and inhibits DNA replication. So we picked the two different anti-cancer drugs, adriamycin and cisplatin, that mainly used in TNBC for further experiments.

To test the idea of multiple resistances by sharing resistance mechanism, anti-cancer drugs were treated to MDA-MB-231 and MDA-MB-231/IR cells and cell viability was detected by MTT assay. Adriamycin treatment significantly decreased the cell viability of MDA-MB-231 in a dose dependent manner. Adriamycin was treated with a range of concentration from 50 to 800 nM and reduced viability of MDA-MB-231 cells from $82.35 \pm 1.59\%$ to $26.98 \pm 2.33\%$. IC 50 value of adriamycin on MDA-MB-231 was 393.33 ± 9.43 nM (Figure 2A). With same range of concentration of adriamycin only diminished MDA-MB-231/IR cells from $104.32 \pm 3.43\%$ to $58.29 \pm 2.04\%$ and IC 50 value on MDA-MB-231/IR was above 800 nM (Figure 2A). Cisplatin affected both MDA-MB-231 and MDA-MB-231/IR cells dose-dependently. Cisplatin was treated with a range of concentration from 6.25 to 100 μ M and reduced viability of MDA-MB-231 cells from $81.07 \pm 3.52\%$ to $6.51 \pm 1.28\%$. IC 50 value of cisplatin on MDA-MB-231 was 22.39 ± 1.61 μ M (Figure 2B). With same range of concentration of cisplatin decreased MDA-MB-231/IR cells from $98.41 \pm$

4.21% to $17.69 \pm 2.10\%$ and IC 50 value on MDA-MB-231/IR cells was $46.44 \pm 2.82 \mu\text{M}$ (Figure 2B).

To certify that MDA-MB-231/IR cells possessed drug resistance, we performed cell cycle analysis by fluorescence activated cell sorting (FACS) to see if the drug treatment changed cell cycle distribution of both cells (Figure 2C, 2D). In basal level, cell cycle distributions of MDA-MB-231 cells and MDA-MB-231/IR cells were not distinguishable. Twenty-four hours of cancer drugs treatment increased the population of cells in sub G1 and G2/M phase in MDA-MB-231 (Figure 2C, 2D). Population in sub G1 increased from $2.43 \pm 0.52\%$ to $11.87 \pm 1.23\%$ after treated with 100 nM of adriamycin on MDA-MB-231 cells whereas population of sub G1 increased from $2.16 \pm 0.11\%$ to $3.81 \pm 1.39\%$ on MDA-MB-231/IR cells (Figure 2E). Cisplatin was treated to MDA-MB-231 cells and MDA-MB-231/IR cells from 50 μM to 200 μM for 24 h. The percentage of cells in sub G1, which indicating dead cells, elevated only in MDA-MB-231 cells as the concentration went by. After treated with 100 μM of cisplatin, sub G1 population increased from $4.01 \pm 0.28\%$ to $10.91 \pm 0.56\%$ on MDA-MB-231 cells while the population of sub G1 did not changed on MDA-MB-231/IR cells (Figure 2F). This indicated that treatment of the cancer drugs induced cell death in MDA-MB-231 cells by increasing sub G1 and apoptosis. To summarize, MDA-MB-231/IR cells presented chemo-resistance along with radio-resistance.

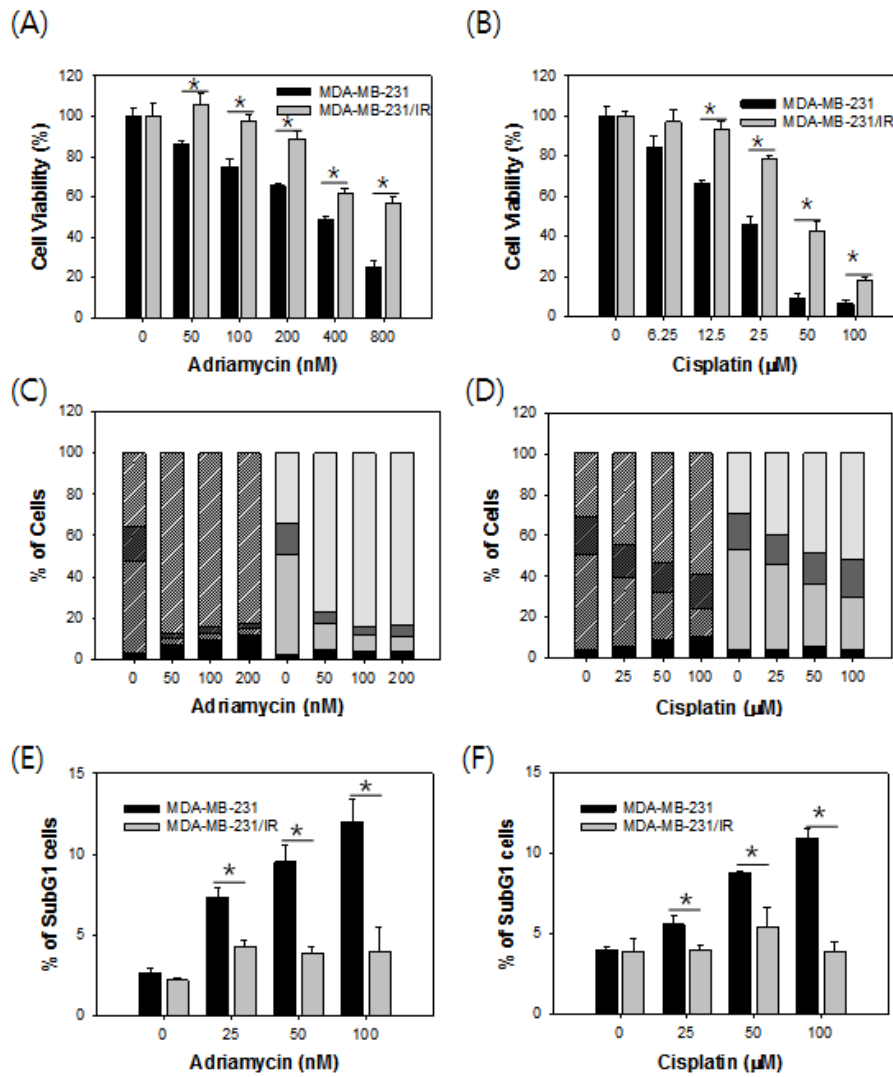


Figure 2. MDA-MB-231/IR developed chemo-resistance compared to parental cell MDA-MB-231. MTT assay of MDA-MB-231 and MDA-MB-231/IR cells treated with adriamycin (50- 800 nM, A) and cisplatin (6.25- 100 μM, B) for 24 h. Cell cycle distribution (diagonal bars: MDA-MB-231, plain bars: MDA-MB-231/IR) and Sub G1 were measured by FACS after adriamycin (C, E) and cisplatin (D, F) treatment for 24 h using PI staining. Values represent means ± standard deviation (SD) (* p < 0.05).

4.3. Chemo- resistance of MDA-MB-231/IR cells evaluated by Annexin V/PI assay

To confirm the chemo-resistance of MDA-MB-231/IR cells, Annexin V/PI assay was performed to detect apoptosis using flow cytometry (Figure 3). Annexin V/PI assay indicates apoptotic cells by detecting fluorescence of antigens binds to annexin V and DNA fragment. The percentage of cells classified as apoptosis increased after treatment of adriamycin and cisplatin in MDA-MB-231 cells following to the increasing concentration.

MDA-MB-231 and MDA-MB-231/IR cells were treated with adriamycin in a range of concentration from 62.5 to 250 nM (Figure 3A, 3B). Percentage of apoptotic cells increased from $7.32 \pm 1.25\%$ to $37.81 \pm 6.55\%$ in MDA-MB-231 while the percentage increased from $6.51 \pm 1.57\%$ to $24.16 \pm 3.81\%$ in MDA-MB-231/IR.

Cells were treated with cisplatin in a range of concentration from 50 to 200 μM (Figure 3C, 3D). Percentage of apoptotic cells increased from $4.29 \pm 0.33\%$ to $16.93 \pm 4.32\%$ in MDA-MB-231 whereas no statistical change was exhibited in percentage of apoptotic cells on MDA-MB-231/IR (from $4.52 \pm 1.35\%$ to $5.32 \pm 1.22\%$). This indicated that adriamycin and cisplatin did not induced apoptosis on MDA-MB-231/IR cells as much as MDA-MB-231 cells. To sum up the results, MDA-MB-231/IR cells had chemo-resistance in adriamycin and cisplatin as well as radio-resistance.

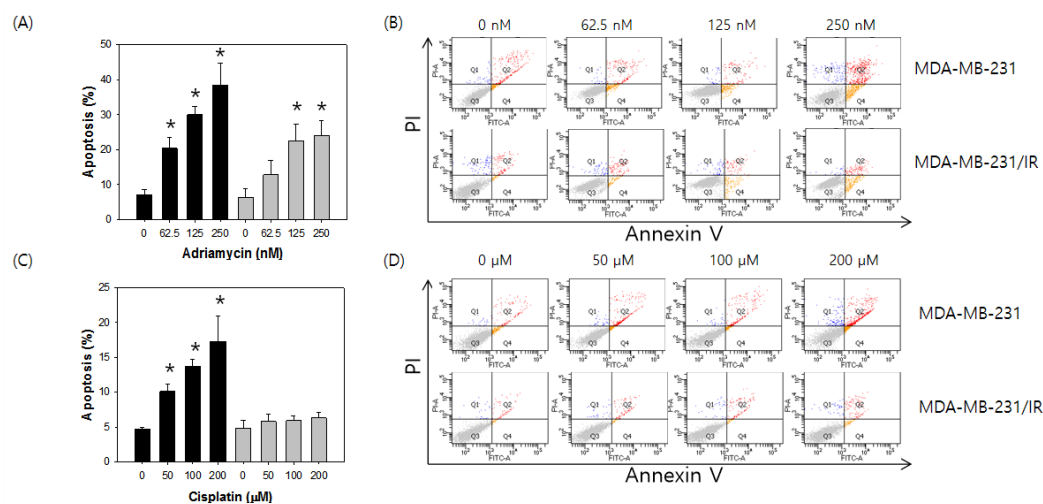


Figure 3. Annexin V/PI assay was performed to investigate chemo- resistance of MDA-MB-231/IR cells. MDA-MB-231 and MDA-MB-231/IR was treated with adriamycin (A, B) and cisplatin (C, D) for 24 h (black bars: MDA-MB-231, gray bars: MDA-MB-231/IR). Values represent means \pm standard deviation (SD) (* $p < 0.05$).

4.4. MDA-MB-231/IR cells exhibited epithelial to mesenchymal morphology compared to parental cells

After generated the resistant cell, we observed and compared the morphology of therapy mimicking cells versus typical MDA-MB-231 cells. Under microscope, MDA-MB-231/IR cells had especially different shape compared to its parental cell MDA-MB-231 (Figure 4A). MDA-MB-231/IR cells exhibited long, spindle-like shaped cell morphology with increased distance between the cells than MDA-MB-231 cells.

As it is known correlation between the change to spindle-like morphology and epithelial to mesenchymal transition (EMT), western blot was carried out to make sure that MDA-MB-231/IR cells had occurred EMT. Vimentin, slug and snail is a well-known protein markers that regulate EMT phenomena. The expression levels of vimentin, slug, and snail increased by 2.94 ± 0.21 , 5.70 ± 0.35 , and 2.12 ± 0.34 fold respectively in MDA-MB-231/IR cells than MDA-MB-231 cells (Figure 4B, 4C). This increased expression of EMT marker proteins were paralleled to our observation under microscope.

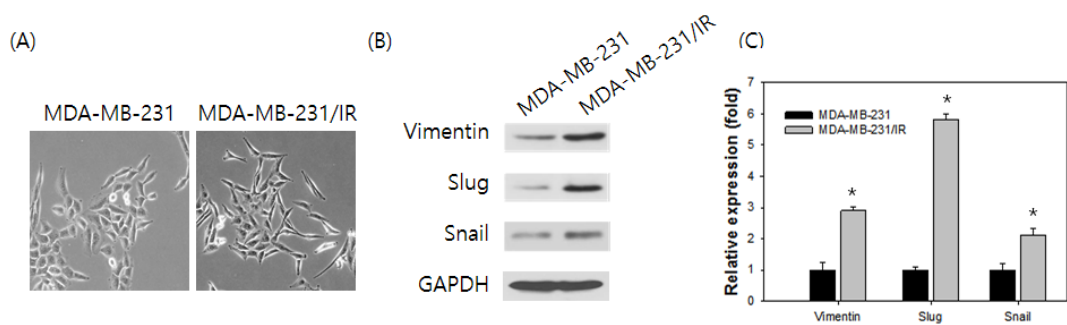


Figure 4. Comparison of MDA-MB-231 and MDA-MB-231/IR cells in morphology and expression of EMT marker proteins. The morphology of MDA-MB-231 and MDA-MB-231/IR was pictured under light microscope (A). Expression levels of EMT-related proteins were analyzed by western blot. As an internal control, glyceraldehyde 3-phosphate dehydrogenase (GAPDH) was used (B). The band intensities were quantified using ImageJ software (C). Values represent means \pm standard deviation (SD) (* $p < 0.05$).

4.5. MDA-MB-231/IR cells exhibited enhanced migration and invasion ability compared to parental cells

Next, we tested whether MDA-MB-231/IR cells had migration ability by wound healing assay to determine that MDA-MB-231/IR cells gained EMT phenotype by 50 Gy of repetitive irradiation. The gap filling rate was determined for 24 h. The $39.55 \pm 2.81\%$ of the gap was closed in MDA-MB-231 cells while $65.85 \pm 3.11\%$ of gap was closed in MDA-MB-231/IR cells (Figure 5A, 5B). The result definitely supported increased spreading and migrating ability of MDA-MB-231/IR cells than MDA-MB-231 cells.

On top of the migration, invasion assay using transwell system was carried out. Only invaded cells to other side of chamber's membrane was collected, fixed and dyed with crystal violet. Compared to MDA-MB-231 cells, 1.48 ± 0.13 fold more MDA-MB-231/IR cells moved through the pores of membrane (Figure 5C, 5D). Migration and invasion assays indicated the metastatic ability has increased in MDA-MB-231/IR cells compared to parental cells.

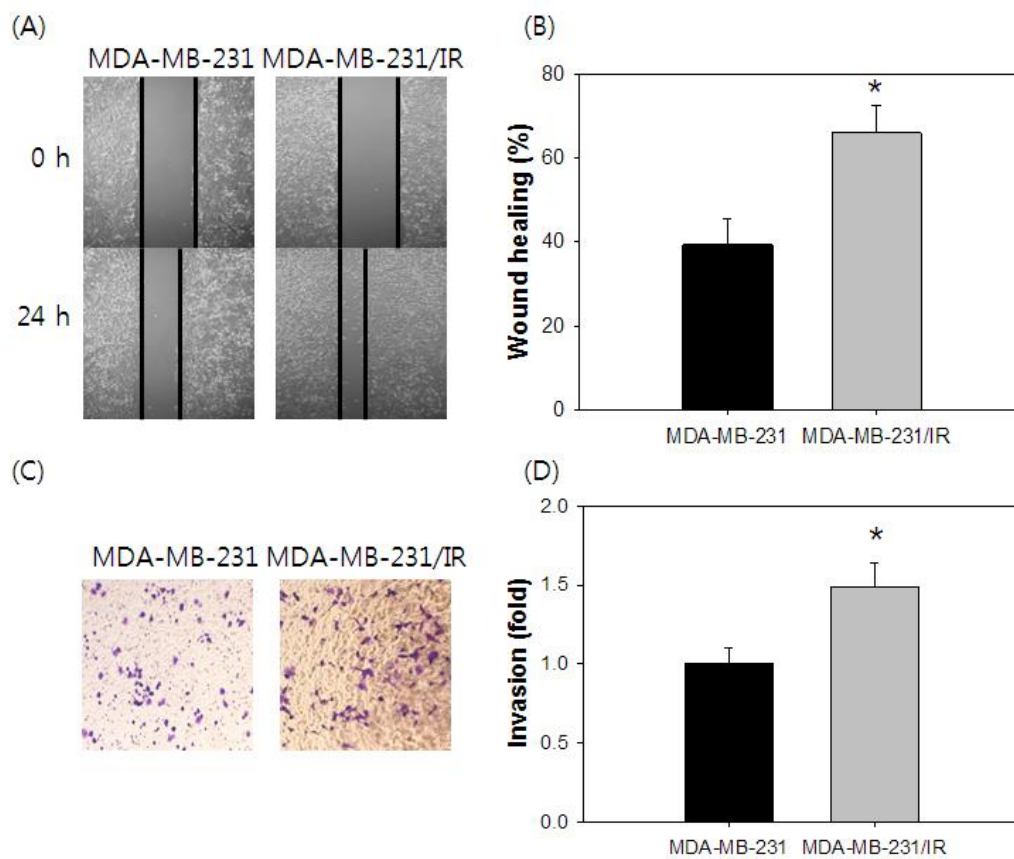


Figure 5. MDA-MB-231/IR cells exhibited enhanced migration and invasion ability compared to parental cells. Wound healing assay of MDA-MB-231 and MDA-MB-231/IR for 24 h (A, B). Invasion assay was performed in MDA-MB-231 and MDA-MB-231/IR for 24 h (C, D). Values represent means \pm standard deviation (SD) (* $p < 0.05$).

4.6. Mammosphere forming ability and expression levels of stem cell-like markers were enhanced in MDA-MB-231/IR cells than those of parental cells

The acquired characteristics of MDA-MB-231/IR cells, such as drug resistance, migration, and invasion, are considered to be tightly correlated with cancer stem cells characteristics, following to other researchers. To examine this hypothesis that MDA-MB-231/IR cells had acquired cancer stem cell property, mammosphere formation assay and western blot assay were conducted.

Mammospheres formed from MDA-MB-231/IR had greater size and more number than MDA-MB-231 (Figure 6A). The average size of mammospheres of MDA-MB-231/IR cells (382.16 pixel) was 2.08-fold greater than the size of MDA-MB-231 cells (183.32 pixel) (Figure 6B). On top of that, MDA-MB-231/IR cells created 1.44-fold more mammosphere than MDA-MB-231 from equal number of single cells (Figure 6C).

Western blot was carried out to qualify stem cell-like characters on MDA-MB-231/IR cells. Stem cell surface markers were detected and MDA-MB-231/IR cells had clearly higher expression in western blot (Figure 6D). The expression levels of CD44 and Oct3/4 increased by 1.56 ± 0.06 and 1.32 ± 0.07 fold in MDA-MB-231/IR than MDA-MB-231. Some researchers had claimed that ATP-Binding cassette (ABC) transporter gave cancer cells stem cell-like character, by effluxing drugs (Scharenberg et al., 2002). So we performed western blot on several ABC transporters. In MDA-MB-231/IR cells, the expression levels of MRP1, ABCG2, and MDR1 were increased by 1.71 ± 0.23 , 1.38 ± 0.07 , and 1.19 ± 0.04 fold respectively than those in MDA-MB-231 cells (Figure 6D, 6E). To sum up, mammosphere forming ability and expression of stem cell-like markers conducted by western blot were enhanced in MDA-MB-231/IR compared to MDA-MB-231.

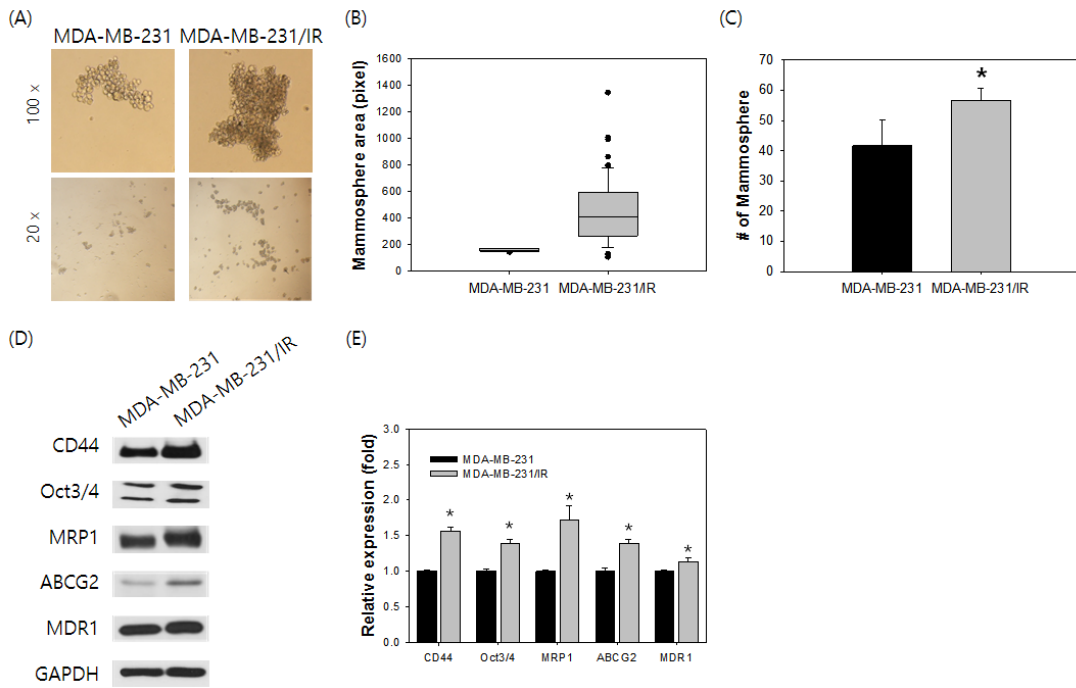


Figure 6. Mammospheres forming ability and expression levels of stem cell-like markers on MDA-MB-231/IR compared to MDA-MB-231. Representative images were captured under light microscope (20x and 100x, A). Size of mammospheres (B) and number of mammospheres (C) were measured by ImageJ software. Western blot was performed for stem cell-like markers (D). The band intensities were quantified using ImageJ software (E). Values represent means \pm standard deviation (SD) (* $p < 0.05$).

4.7. MDA-MB-231/IR cells exhibited stem cell-like characters compared to its parental cells

To scrutinize on the aspect of stem cell-like property, FACS was utilized to detect the expression of cell surface markers of CD44 and CD24 conjugated with FITC and PE. MDA-MB-231 cells have been reported to have higher CD44^{high} and CD24^{low} cell population (Q1) among breast cancer cells. According to Li et al., MDA-MB-231 had 99.1% of cells in Q1 while MCF7 had 0.9% of cells in Q1. The Q1 populations of SK-BR-3 and MDA-MB-468 cells were also measured, however, no cell was observed in Q1 (Li et al., 2017). MDA-MB-231/IR cells showed slightly higher Q1 population compared to their parental cells (Figure 7A, 7B). The percent of cells in Q1 population was $90.05 \pm 2.35\%$ in MDA-MB-231/IR whereas $84.98 \pm 4.72\%$ in MDA-MB-231. This result explained that both MDA-MB-231 and MDA-MB-231/IR cells had high percentage of CD44^{high} and CD24^{low} population.

It is also reported that cells classified as side population (SP) could be regarded as stem cells, so that we carried out an assay to detect side population by using Hoechst 33342. SP assay is using one of the characters of stem cell is the ability to pump out materials including drugs and dyes. The percentages of SP in MDA-MB-231 cells and MDA-MB-231/IR cells were $1.52 \pm 0.43\%$ and $2.62 \pm 0.38\%$, respectively (Figure 7C, 7D). It revealed that the percentage of SP in MDA-MB-231/IR cells increased by 1.72 ± 1.13 fold compared to parental MDA-MB-231 cells. In conclusion, the results illustrated that MDA-MB-231/IR cells gained more stem-like property than the parental cells while repetitive radiations as well as drug- and radio-resistance.

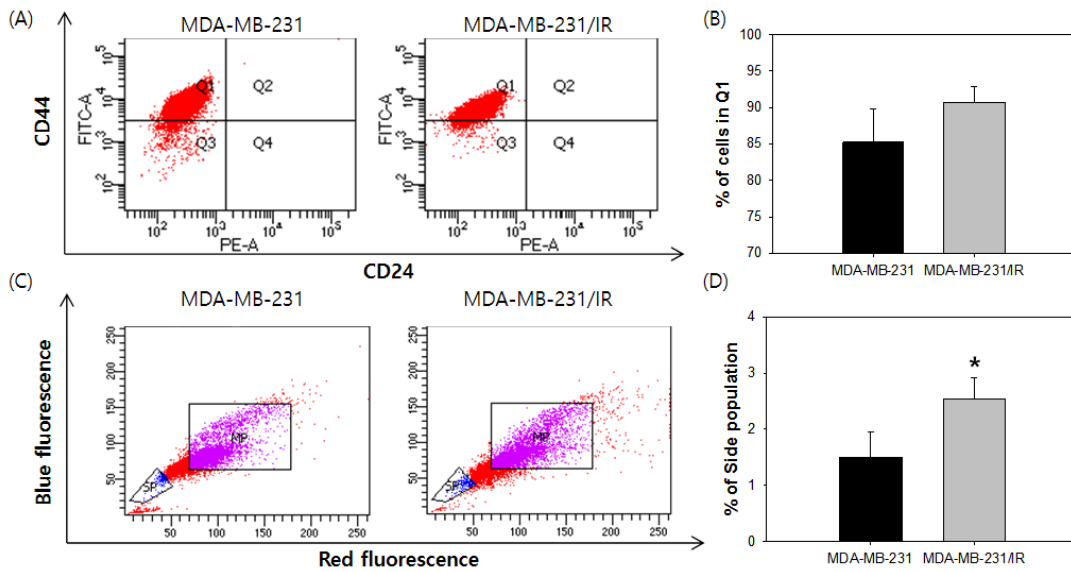


Figure 7. MDA-MB-231/IR cells exhibited stem cell-like characters compared to its parental cells. CD44^{high} and CD24^{low} population (Q1, upper left quadrant) was determined by CD44-FITC and CD24-PE antigens after 15 min of incubation at 37°C (A, B). Side population was detected after 1.5 h of incubation with Hoechst 33342 dye at 37°C (C, D). Side population was displayed in blue and main population was displayed in purple. Values represent means \pm standard deviation (SD) (* $p < 0.05$).

4.8. Transcriptomics analysis on MDA-MB-231/IR cells

To gain a better understanding of chemo- and radio- resistance, we conducted RNA-seq to identify differentially expressed genes (DEGs). Total 31,498 transcripts were identified in this study. In comparison to the gene expression profiles for MDA-MB-231 cells, we found that 39 DEGs were up-regulated and 38 DEGs were down-regulated than MDA-MB-231/IR cells ($P < 0.001$, supplementary table 1, 2).

We used DAVID (version 6.8) to visualize the gene regulatory network and pathways and Gene Ontology to understand how radiation affects the MDA-MB-231 cell lines transcriptional gene network. From our analysis, we observed NF- κ B signaling pathway (11%), TNF signaling pathway (10%), Toll-like receptor signaling pathway (10%) were highly regulated (Figure 8A). Gene ontology analysis revealed the biological process including regulation of cell division (11%), transcription from RNA polymerase II promoter (22%), and protein phosphorylation (11%) (Figure 8B). Gene ontology cellular component analysis explains further focal adhesion (12%), nucleoplasm (26%), cytoplasm (39%), and membrane (16%) were activated in the resistance cells (Figure 8C). ATP (56%), chromatin (22%), and interleukin-1 (IL-1) receptor (11%) binding are other molecular process highly regulated (Figure 8D). Taken together, we performed pathway analysis to identify the enriched pathways from DEGs and GO analysis to find up and down regulated genes biological function and molecular process.

Pathway and GO analysis with DEGs from MDA-MB-231/IR cells

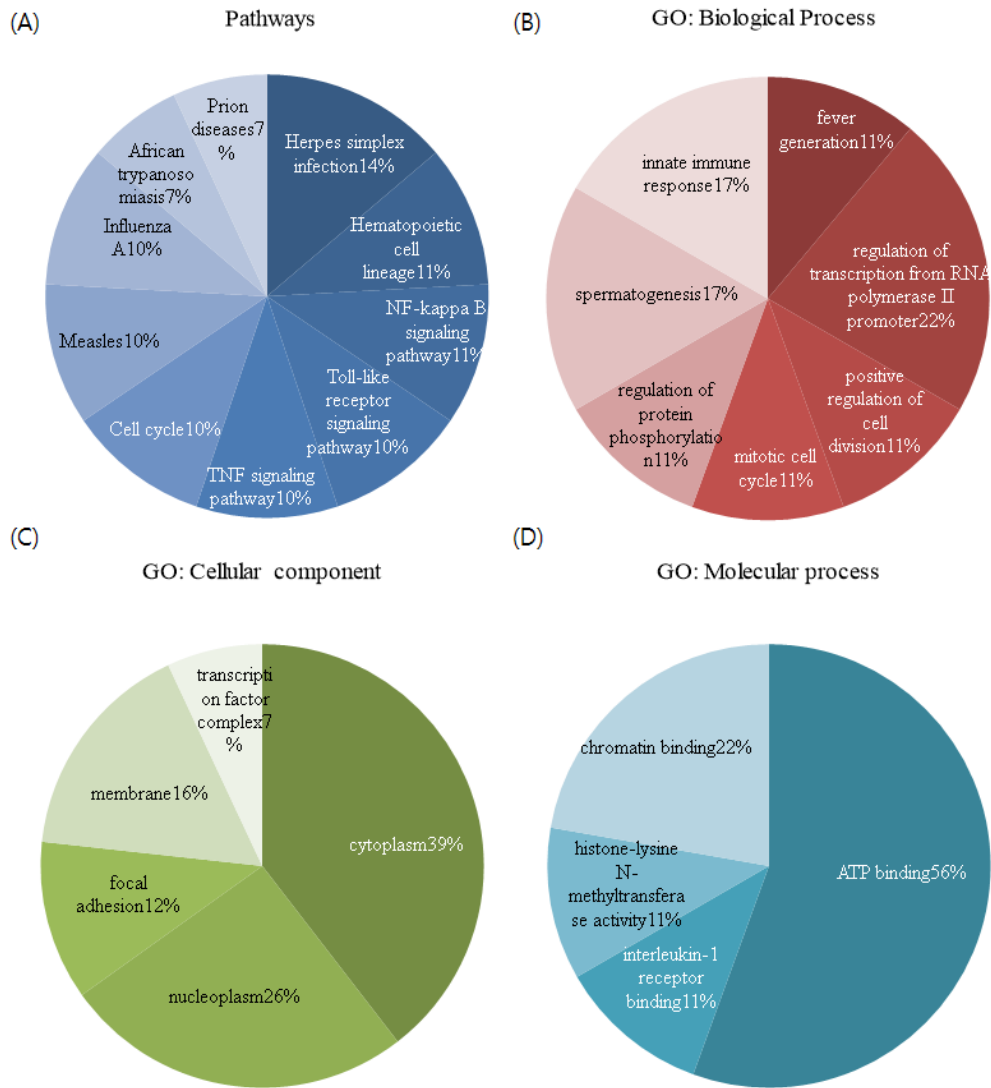


Figure 8. Pathway and Gene Ontology analysis with differentially expressed genes (DEGs) of MDA-MB-231/IR cells compared to MDA-MB-231 cells. Pathway analysis (A) and Gene ontology (GO) analysis (B, C, and D) of DEGs of MDA-MB-231/IR cells compared to MDA-MB-231.

4.9. Cancer resistance was reported in 12 DEGs of MDA-MB-231/IR

To identify roles of those genes in cancer resistance, a literature search was carried out and 24 genes were identified to be associated with cancer resistance according to previous reports. Twelve genes that met our standard (difference >10 in up-regulated genes and difference $<(-4)$ in down-regulated genes) were selected: AKR1C1, FTL, MK, LG3BP, GFPT2, TGFBI, AKR1C3, CCDC69, AKR1C2, TWF1, PKP3, and IFIT2. We named the 12 genes as cancer resistance genes. The difference in expression levels and fold change of the genes are shown in Table 1 and their expressions were confirmed by quantitative realtime PCR in figure 9. The expression levels of genes quantified by realtime PCR were different from fold changes in transcriptomic analysis. The expression levels of AKR1C1, AKR1C2, TGFBI, LGS3B, AKR1C3, MK, GFPT2, FTL, CCDC69, TWF1, IFIT2 and PKP3 were described in log₂ fold change (Figure 9B).

Table 1. Cancer resistance genes from DEGs of MDA-MB-231/IR cells are described in difference, fold (log 2), and their functions.

No.	Difference	Fold (log2)	Gene	Full name	Role in cancer	References
1	97.57	6.83	AKR1C1	Aldo-keto reductase 1C1	Metastasis	Zhu et al., 2018
2	79.67	6.64	FTL	Ferritin Light Chain	Drug resistance	Li et al., 2014
3	77.43	2.92	MK	Midkine	Metastasis	Sun et al., 2017
4	62.20	6.01	LG3BP	Galectin-3-binding protein	Anti-differentiation	White et al., 2015
5	46.92	3.04	GFPT2	Glutamine-Fructose-6-Phosphate Transaminase 2	Metabolism	Simpson et al., 2012
6	42.64	3.34	TGFBI	Transforming Growth Factor Beta Induced	Metastasis	Ma et al., 2008
7	42.35	3.87	AKR1C3	Aldo-keto reductase 1C3	Drug resistance	Liu et al., 2015
8	37.59	2.96	CCDC69	Coiled-Coil Domain Containing 69	Drug resistance	Cui et al., 2017
9	14.51	4.13	AKR1C2	Aldo-keto reductase 1C2	Metastasis	Buranrat et al., 2015
10	12.55	Inf	TWF1	Twinfilin Actin Binding Protein 1	Migration	Bockhorn et al., 2013
11	-4.33	-Inf	PKP3	Plakophilin 3	Invasion	Takahashi et al., 2012
12	-85.90	-2.84	IFIT2	Interferon induced protein with tetratricopeptide repeats 2	Apoptosis mediator	Chen et al., 2018

Inf: infinity, the expression of the gene was not determined.

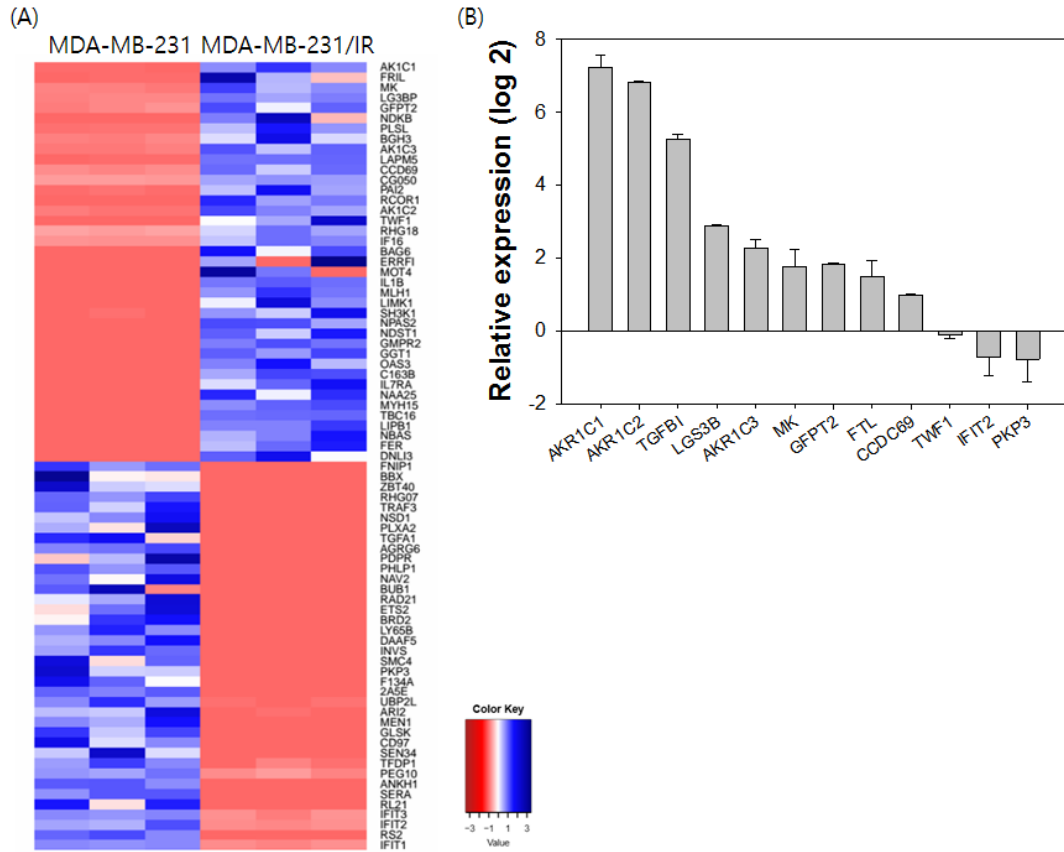


Figure 9. Analysis of DEGs in MDA-MB-231/IR cells compared to MDA-MB-231 cells. Heatmap of gene expression data are shown in relative transcription levels of triplicate (A). Quantitative realtime PCR of cancer resistance genes in DEGs of MDA-MB-231/IR (B).

4.10. Baicalein effectively targeted chemo- and radio-resistance MDA-MB-231/IR cells

Researchers look for another ways to kill the cancer cells beyond conventional therapy to target therapy-resistant breast cancer (Hui et al., 2013). Phytochemicals are chemicals from plants and many of those are known to be benevolent to human health, including anti-cancer effect. We conducted a research to narrow groups of phytochemicals that have anti-cancer effect in breast cancer. There were compelling researches that polyphenols and flavonoids, including flavones and flavonols, are reported to be active chemicals against breast cancer cells. We searched for phytochemicals that were reported to have effects on breast cancer cells, and 3 phenolics, 3 flavones, and 4 flavonols were found (Bauer et al., 2017; Wang et al., 2010; Lee et al., 2005; Kim et al., 2008; Rodgers et al., 1998; Iriti et al., 2017; Lakshmi et al., 2014; Choi et al., 2018; Yin et al., 2009). Those phytochemicals were tested for cell viability assay to target therapy resistance MDA-MB-231/IR cells as well as MDA-MB-231 cells.

We conducted MTT assay for the test cytotoxic effect of 10 phytochemicals that were available (Table 2). Among the phytochemicals we tested, apigenin, baicalein, catechol, and myricetin were found to have IC 50 values in both cells within the tested concentration (0 - 200 μ M). IC 50 values of apigenin, baicalein, catechol, and myricetin on MDA-MB-231 cells were 75.12 ± 1.85 , 44.25 ± 2.47 , 185.21 ± 3.69 , and 30.29 ± 1.87 μ M, respectively. IC 50 values of the phytochemicals on MDA-MB-231/IR cells were 83.11 ± 4.01 , 38.58 ± 2.86 , 92.16 ± 1.98 , and 78.61 ± 1.97 μ M, respectively. Phytochemicals without IC 50 values on both cells were ejected for further experiment. As baicalein could efficiently target the both cells with lowest concentration within the compounds we tested, we recruited baicalein for further experiments.

Table 2. IC 50 concentrations of each phytochemical on MDA-MB-231 and MDA-MB-231/IR.

No.	Group	Phytochemical	IC 50 (μ M)	
			MDA-MB-231	MDA-MB-231/IR
1		Apigenin	75.12 \pm 1.85	83.11 \pm 4.01 *
2	Flavone	Baicalein	44.25 \pm 2.47	38.58 \pm 2.86 *
3		Tangeretin	>200	>200
4		Kaempferol	>200	198.52 \pm 5.12
5	Flavonol	Myricetin	30.29 \pm 1.87	78.61 \pm 1.97 *
6		Quercetin	>200	167.43 \pm 2.37 *
7		Rutin	>200	>200
8		Catechol	185.21 \pm 3.69	92.16 \pm 1.98 *
9	Phenol	Chlorogenic acid	>200	183.66 \pm 3.10 *
10		Protocatechuic acid	>200	>200

Values represent means \pm standard deviation (SD) (* p < 0.05).

4.11. Baicalein reversed expression of IFIT2 in MDA-MB-231/IR

As baicalein was found to be a competitive phytochemical which could target breast cancer cells MDA-MB-231/IR, time- and dose- dependent viability assay on MDA-MB-231/IR cells after baicalein treatment was carried out. As the concentration or the treatment time went by, the viability of MDA-MB-231/IR significantly decreased (Figure 10A). Cell viability of MDA-MB-231/IR decreased from 78.24 ± 2.54 to $16.72 \pm 0.11\%$ after 24 h of baicalein treatment (20-100 μM). Cell viabilities of MDA-MB-231/IR were diminished by 102.11 ± 9.82 , 98.03 ± 2.28 , and $43.25 \pm 3.93\%$ after treated with 40 μM of baicalein for 6, 12, and 24 h. We hypothesized that baicalein can kill MDA-MB-231/IR cell by targeting cancer resistance genes that were detected by transcriptomics analysis. With 12 of cancer resistance genes we identified from transcriptomic analysis, we performed realtime-PCR to figure out if baicalein could reverse the expression within the genes. Since their expression is tightly connected to cancer resistance, we thought that baicalein could also convert the gene expression level compared to the level of MDA-MB-231 cells, from higher to lower level or vice versa. The expression levels of cancer resistance genes were measured by quantitative realtime PCR with or without a range of baicalein treatment (10- 80 μM) (Figure 10B). Only the expression of IFIT2 has changed among 12 cancer resistance genes; the expression was lower (0.63 ± 0.09 fold) than MDA-MB-231 in the condition without baicalein treatment but it has risen to 1.86-fold after 80 μM of baicalein treatment (1.82 ± 0.39 fold) (Figure 10C). The mRNA expression of IFIT2 increased baicalein treatment dose-dependently. Taken together, baicalein target MDA-MB-231/IR cells while reversing the expression of one of the cancer resistance genes, IFIT2.

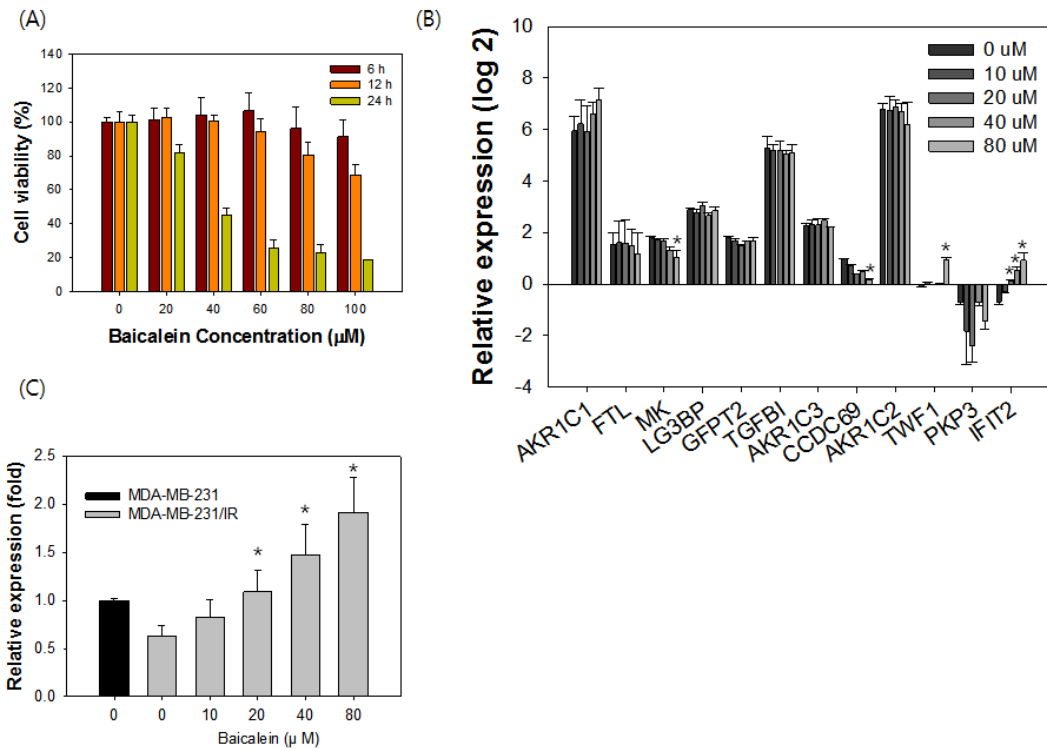
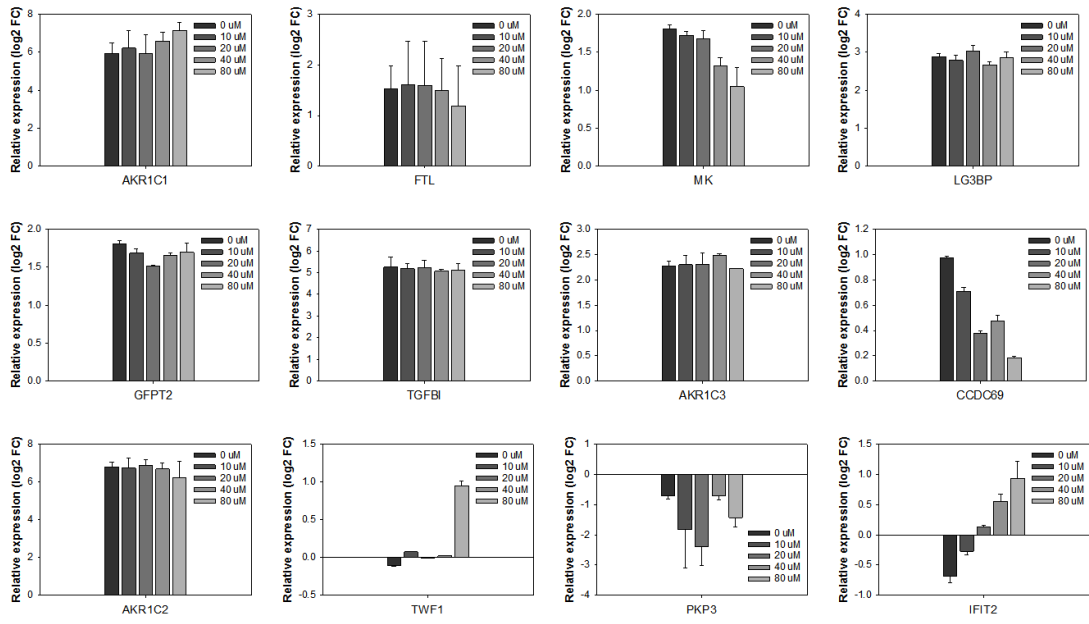


Figure 10. Baicalein treatment reversed mRNA expression level of MDA-MB-231/IR. MTT assay on MDA-MB-231/IR treated with a range of baicalein (20-100 μM) for 6, 12, and 24 h (A). Expression levels of 12 cancer resistance genes (shown in log₂ fold change) on MDA-MB-231/IR were measured by quantitative realtime PCR after treated with a range of baicalein for 24 h (B). The expression level of IFIT2 was described in fold change (C). Values represent means ± standard deviation (SD) (* p < 0.05).



(continued) Figure 10D. Relative expressions of 12 cancer resistance gene after 24 h of baicalein treatment (shown in log₂ fold change).

4.12. Baicalein reduced protein expression level of Slug

It is confirmed that baicalein treatment on MDA-MB-231/IR, we tried to find that the baicalein treatment could reverse the characters of MDA-MB-231/IR cells. As we tested above, MDA-MB-231/IR cells have been shown EMT characteristics higher than its original cells. After treating different concentration of baicalein, we tested whether the treatment could change them.

To figure out the change of phenotype to EMT of MDA-MB-231/IR cells, western blot of EMT markers was carried out after baicalein treatment (10, 20 μM) (Figure 11A). The protein expressions of Slug and Snail on MDA-MB-231/IR were higher compared to those of MDA-MB-231 cells. While the protein expression of Snail did not changed after 10 and 20 μM of baicalein treatment, the expression of Slug was greatly changed following to baicalein treatment. Twenty μM of baicalein diminished the expression level of Slug by 0.65 ± 0.02 fold after 24 h (Figure 11B). The reduced expression level of Slug indicated the possibility of diminished EMT phenomena.

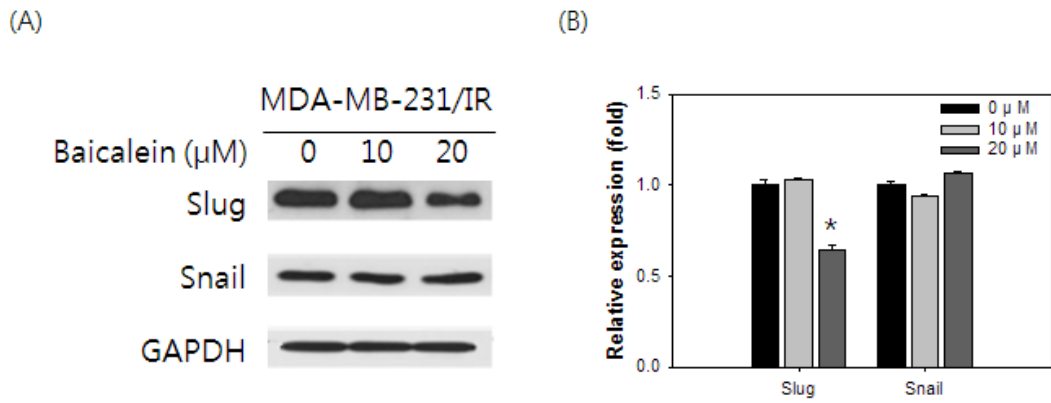


Figure 11. Baicalein reduced expression level of Slug. Western blot of EMT markers on MDA-MB-231 and MDA-MB-231/IR treated with or without baicalein treatment (10, 20 μM) after 24 h. The band intensities were quantified using ImageJ software (B). Values represent means \pm standard deviation (SD) (* $p < 0.05$).

4.13. Baicalein inhibited EMT capacity of MDA-MB-231/IR

Wound healing assay was conducted after 10 and 20 μM of baicalein treatment for 24 h to demonstrate the effect of baicalein on EMT phenomena on MDA-MB-231/IR cells (Figure 12A). Ten and 20 μM of baicalein treatment reduced the wound closure rate of MDA-MB-231/IR cells by 0.84 ± 0.03 and $0.61 \pm 0.05\%$ compared to the cells without baicalein treatment (Figure 12B). On top of the wound healing assay, invasion assay with transwell system was carried out after 24 h of baicalein treatment (Figure 12C). Compared to cells without baicalein treatment, 5, 10, and 20 μM of baicalein treatment decreased the invasion of MDA-MB-231/IR cells by 0.78 ± 0.22 , 0.65 ± 0.27 , and 0.43 ± 0.19 fold, respectively (Figure 12D).

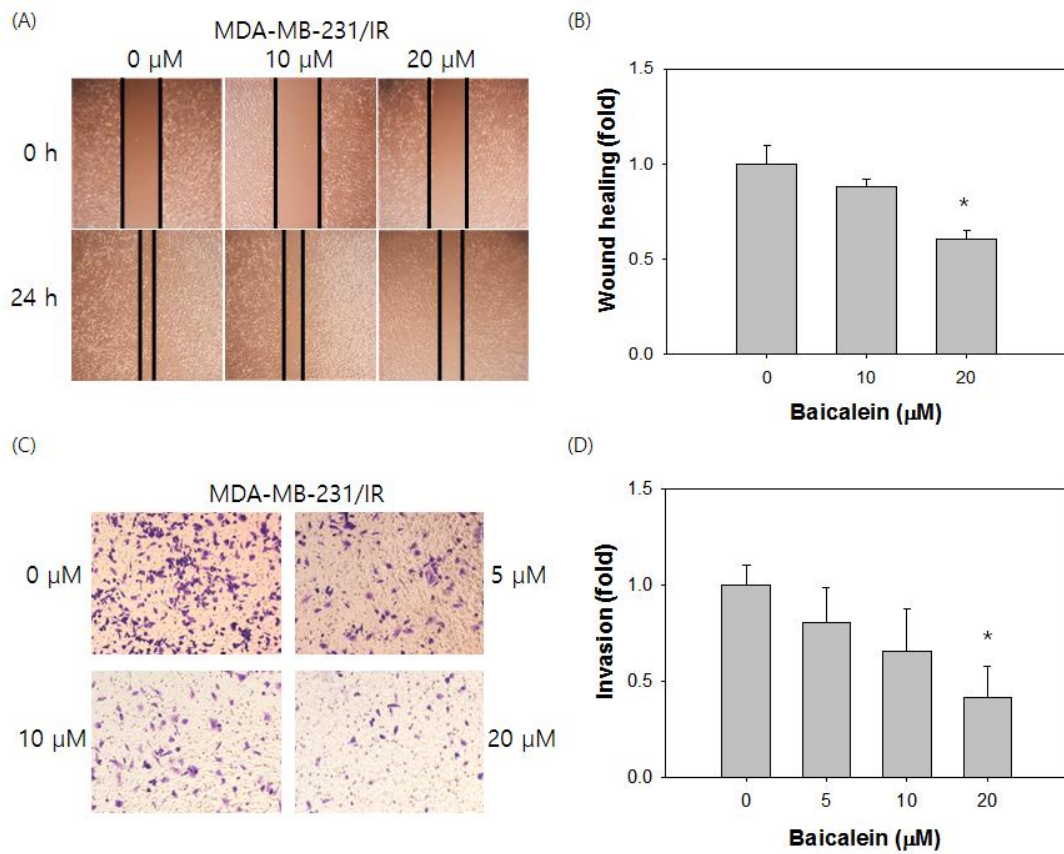


Figure 12. Baicalein treatment inhibited EMT capacity of MDA-MB-231/IR. Wound healing assay on MDA-MB-231/IR treated with or without baicalein 10 or 20 μM for 24 h (A, B). Invasion assay on MDA-MB-231/IR treated with or without baicalein 5, 10, or 20 μM for 24 h (C, D). Values represent means ± standard deviation (SD) (* p< 0.05).

4.14. Baicalein diminished the mammosphere formation and expression of marker proteins in MDA-MB-231/IR

Stem cell-like characters are one of the characteristic features of MDA-MB-231/IR cells in comparison with MDA-MB-231 cells. Mammosphere formation was used to examine the stem cell markers of MDA-MB-231/IR cells after baicalein treatment. The size of the mammospheres of MDA-MB-231/IR cells shrunk as baicalein concentration increased (Figure 13A). The number of mammosphere was also reduce from $56.24 \pm 2.56\%$ to $12.27 \pm 6.31\%$ by 5 to 20 μM of baicalein treatment (Figure 13B).

To examine the stem cell-like character with or without baicalein treatment, western blot was performed. The expression of stem cell-like character markers, ABCG2 and Oct3/4, which were highly expressed in MDA-MB-231/IR decreased after 20 to 80 μM of baicalein treatment (Figure 13C). The expression levels of Oct3/4 and ABCG2 diminished from 0.52 ± 0.04 to 0.19 ± 0.02 fold and from 0.94 ± 0.07 to 0.46 ± 0.03 fold after baicalein treatment (40 to 80 μM) (Figure 13D). Baicalein inhibited stem cell-like characteristics of MDA-MB-231/IR.

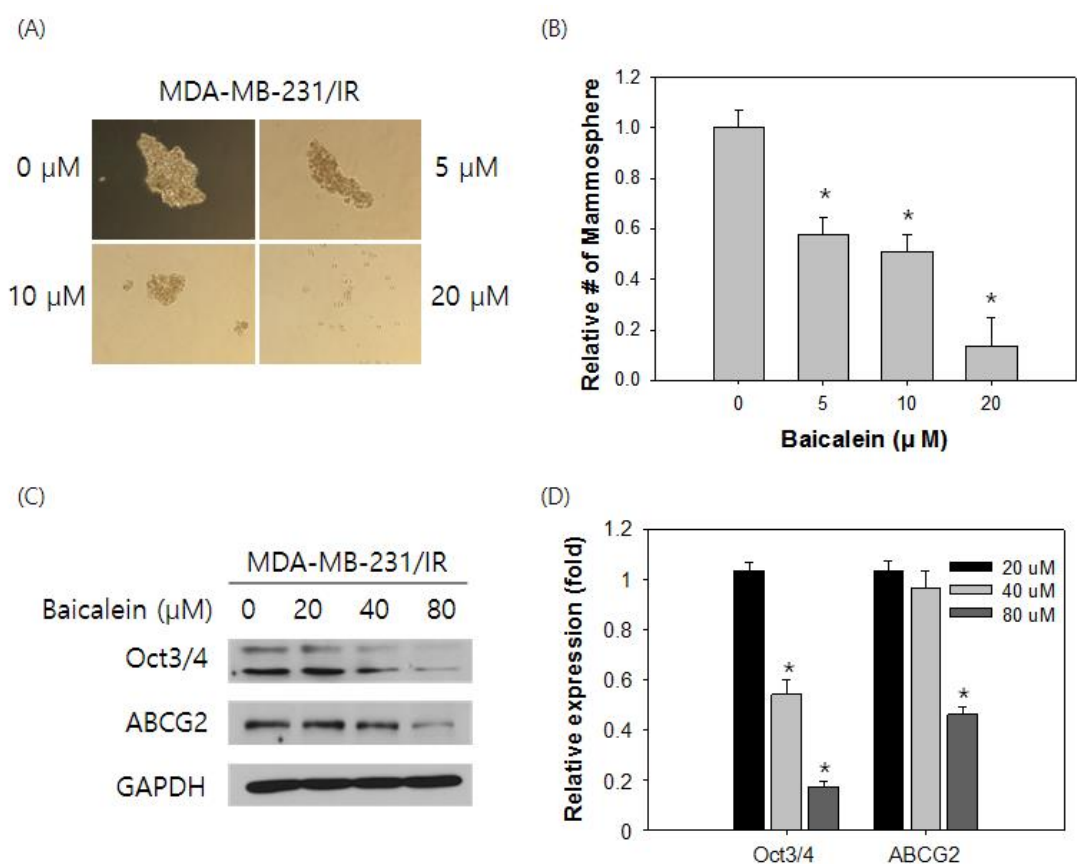


Figure 13. Baicalein treatment diminished mammosphere formation and expression of stem cell-like marker proteins in MDA-MB-231/IR. Mammosphere formation of MDA-MB-231/IR after 24 h of baicalein treatment (5 to 20 μM) (A). The number of mammosphere was measured by ImageJ software (B). Expressions of Oct3/4 and ABCG2 after 24h of baicalein treatment (20 to 80 μM) (C). The band intensities were quantified using ImageJ software (D). Values represent means ± standard deviation (SD) (* p < 0.05).

4.15. Baicalein diminished the stem cell-like characters of MDA-MB-231/IR

For FACS analysis, the distributions of cell surface markers on MDA-MB-231/IR cells were measured after baicalein treatment. The percentage of CD44^{high} and CD24^{low} cells (Q1) was diminished following to reduction of CD44 expression after baicalein treatment (Figure 14A). Baicalein treatment (from 20 to 80 μ M) decreased the population of Q1 from 0.95 ± 0.03 to 0.57 ± 0.08 fold after 24 h (Figure 14B). SP assay using Hoechst 33342 was also conducted after baicalein treatment (Figure 14C). The percentage of SP was also decreased by 0.50 ± 0.03 , 0.46 ± 0.03 , and 0.37 ± 0.02 fold after baicalein treatment of 20, 40, and 80 μ M (Figure 14D). To sum up, baicalein treatment on MDA-MB-231/IR reduced stem cell-like properties of MDA-MB-231/IR cells.

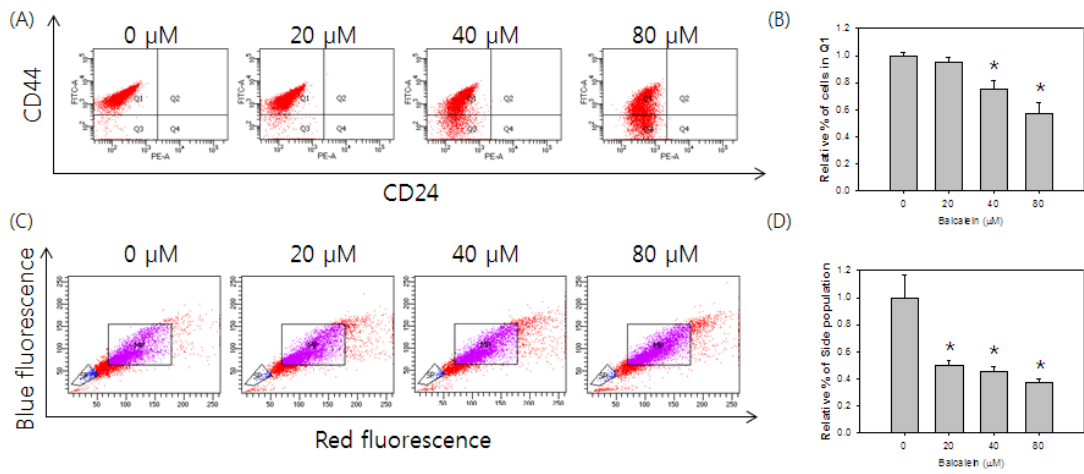


Figure 14. Baicalein diminished stem cell-like characters of MDA-MB-231/IR. CD44^{high} and CD24^{low} population (Q1, upper left quadrant) was determined by CD44-FITC and CD24-PE antigens after 15 min of incubation at 37°C (A, B). Side population was detected after 1.5 h of incubation with Hoechst 33342 dye at 37°C (C, D). Side population was displayed in blue and main population was displayed in purple. Values represent means \pm standard deviation (SD) (* $p < 0.05$).

4.16. Baicalein increased expression levels of apoptosis-related proteins on MDA-MB-231/IR

Baicalein was known to kill cancer cells through apoptosis, so we carried out several experiments to confirm that MDA-MB-231/IR cells could be affected by baicalein in apoptosis. We prepared western blot to detect apoptosis markers when baicalein was treated on MDA-MB-231/IR. The expression of IFIT2 and several apoptosis-related antigens were utilized. For apoptosis, the expression of γ -H2A histone family member X (γ -H2AX), Bax, cleaved (C) - caspase 3 and cleaved (C) - poly (ADP-ribose) polymerase (PARP) were detected by western blot. DNA damage was measured using gamma-H2AX, proapoptotic marker Bax, and activation of apoptosis indicators caspase 3 and PARP were evaluated by the analysis. Protein expressions of IFIT2 and apoptosis markers have increased by baicalein treatment in dose dependent manners (Figure 15A). Baicalein treatment from 10 to 80 μ M increased the expression level of IFIT2 ($\sim 28.24 \pm 0.90$ fold), gamma-H2AX ($\sim 5.47 \pm 0.91$ fold), Bax ($\sim 4.20 \pm 0.67$ fold), C-caspase3 ($\sim 4.20 \pm 0.90$ fold), and C-PARP ($\sim 5.23 \pm 0.95$ fold) (Figure 15B).

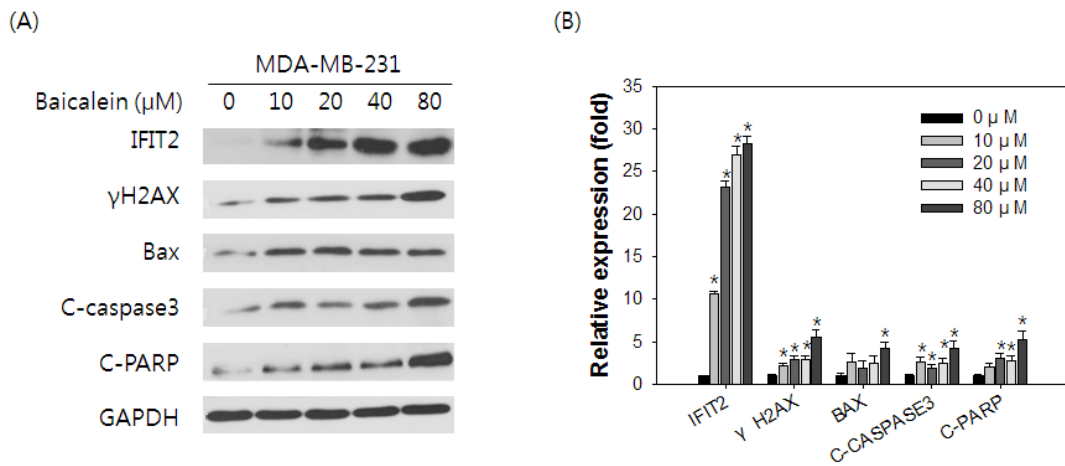


Figure 15. Baicalein increased expression levels of apoptosis-related proteins on MDA-MB-231/IR. Representative of western blot on MDA-MB-231 and MDA-MB-231/IR treated with or without baicalein 10 to 80 μM (A). The band intensities were quantified using ImageJ software (B). Values represent means \pm standard deviation (SD) (* $p < 0.05$).

4.17. Baicalein induces apoptosis on MDA-MB-231/IR cells

The results of Annexin V/PI binding assay demonstrated that baicalein induced apoptosis following to its concentration went by (Figure 16A). Percent of cells in apoptosis had elevated from $7.48 \pm 3.42\%$ to $22.53 \pm 5.21\%$ times after 24 h baicalein treatment from 20 to 80 μM (Figure 16B). Cell cycle analysis also indicated that baicalein treatment from 20 to 80 μM increased sub G1 population from 4.58 ± 1.53 to $14.28 \pm 0.41\%$ (Figure 16C).

To scrutinize the apoptosis occurred in MDA-MB-231/IR cells, JC-1 staining was performed by FACS analysis to investigate changes of mitochondrial membrane potential. As concentration of baicalein increased from 10 to 80 μM , we observed a shift from red to green fluorescence, indicating the mitochondrial membrane depolarization. The ratio green versus red fluorescence increased from $8.32 \pm 3.51\%$ to $23.24 \pm 4.81\%$ (Figure 16D). This result indicates that baicalein kills MDA-MB-231/IR cells in apoptosis by decreasing membrane potential of mitochondria. According to previous reports (Stawowczyk et al., 2011), IFIT2 is also reported to induce apoptosis through lowering mitochondrial membrane potential and we hypothesized that baicalein- induced apoptosis through intrinsic pathway has mediated through increasing the protein expression of IFIT2.

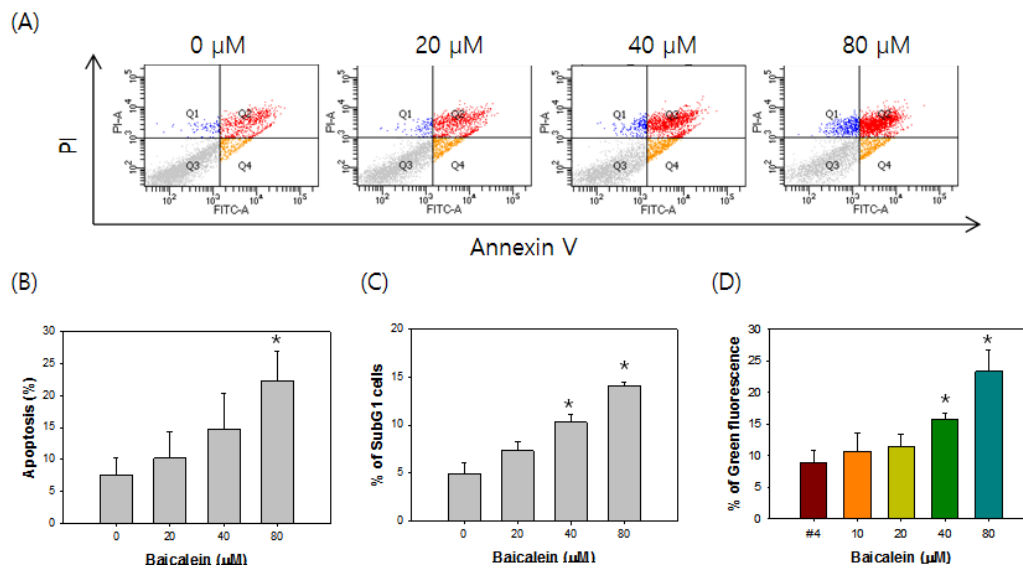


Figure 16. Baicalein induces apoptosis on MDA-MB-231/IR cells. Annexin V/PI assay on MDA-MB-231/IR treated with or without baicalein 20 to 80 μM for 24 h (A, B). Population in sub G1 on MDA-MB-231/IR with or without baicalein 20 to 80 μM for 24 h (C). JC-1 assay on MDA-MB-231/IR with or without baicalein 10 to 80 μM for 24 h (D). Values represent means ± standard deviation (SD) (* p < 0.05).

4.18. Baicalein co-treatment reversed radio- resistance in MDA-MB-231/IR

As baicalein treatment killed the radio- resistance cells and increased the transcriptional and protein expressions of IFIT2, we performed assays to find if this phytochemical can reverse resistance property of cells.

Combination treatment of baicalein with radiation was performed by clonogenic assay. Ten μM of baicalein treatment decreased colony formation of MDA-MB-231/IR cells (Figure 17A). After 2 and 4 Gy of irradiation, 10 μM of baicalein reduced the surviving fraction from 0.94 to 0.54 and from 0.67 to 0.18 (Figure 17B).

In conclusion, baicalein treatment with irradiation exhibited that the combined treatment increased the effects of radiation treatments on radio- resistant MDA-MB-231/IR cells.

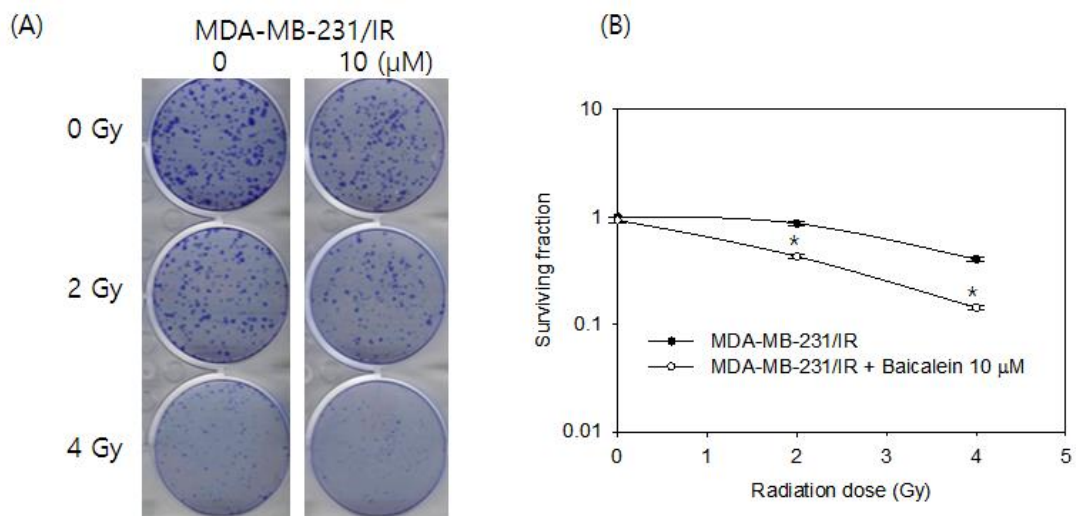


Figure 17. Baicalein co-treatment reversed radio-resistance in MDA-MB-231/IR cells. Representative image of clonogenic assay on MDA-MB-231/IR after 2 and 4 Gy of irradiation with or without 10 μM of baicalein treatment (A). Surviving fraction calculated from numbers of colonies on Figure 17A counted by NICE (B). Values represent means ± standard deviation (SD) (* $p < 0.05$).

4.19. Baicalein co-treatment reversed chemo- resistance in MDA-MB-231/IR

We co-treated baicalein with several anti-cancer drugs for MTT assay. The combination index (CI) value was calculated by software Calcsyn (Biosoft, UK), which offers synergistic effects of the two different treatments in 3 different categories: additive (CI value = 1), synergism (CI value < 1), or antagonism (CI value > 1).

When 5 to 20 μM of baicalein were treated with drugs, the viability of MDA-MB-231/IR cells decreased compared to viabilities of single treatment of baicalein or anti-cancer drugs. Co-treatment of baicalein and adriamycin gave CI values less than 1 in tested combinations generally (Figure 18A). Especially, co-treatment with 20 μM of baicalein and 100 nM of adriamycin exhibited the lowest CI value (0.40) in this combinations which interpreted as synergism (Figure 18A). Co-treatment of baicalein with cisplatin was conducted by MTT assay (Figure 18C). Co-treatment of baicalein and cisplatin gave CI values less than 1 when 10 to 15 μM of baicalein was treated (Figure 18D). Combination of 15 μM of baicalein with 40 μM of cisplatin displayed the lowest CI value (0.32) in this co-treatment.

As a results, baicalein treatment with anti-cancer drugs exhibited synergistic effect on chemo- resistant MDA-MB-231/IR cells.

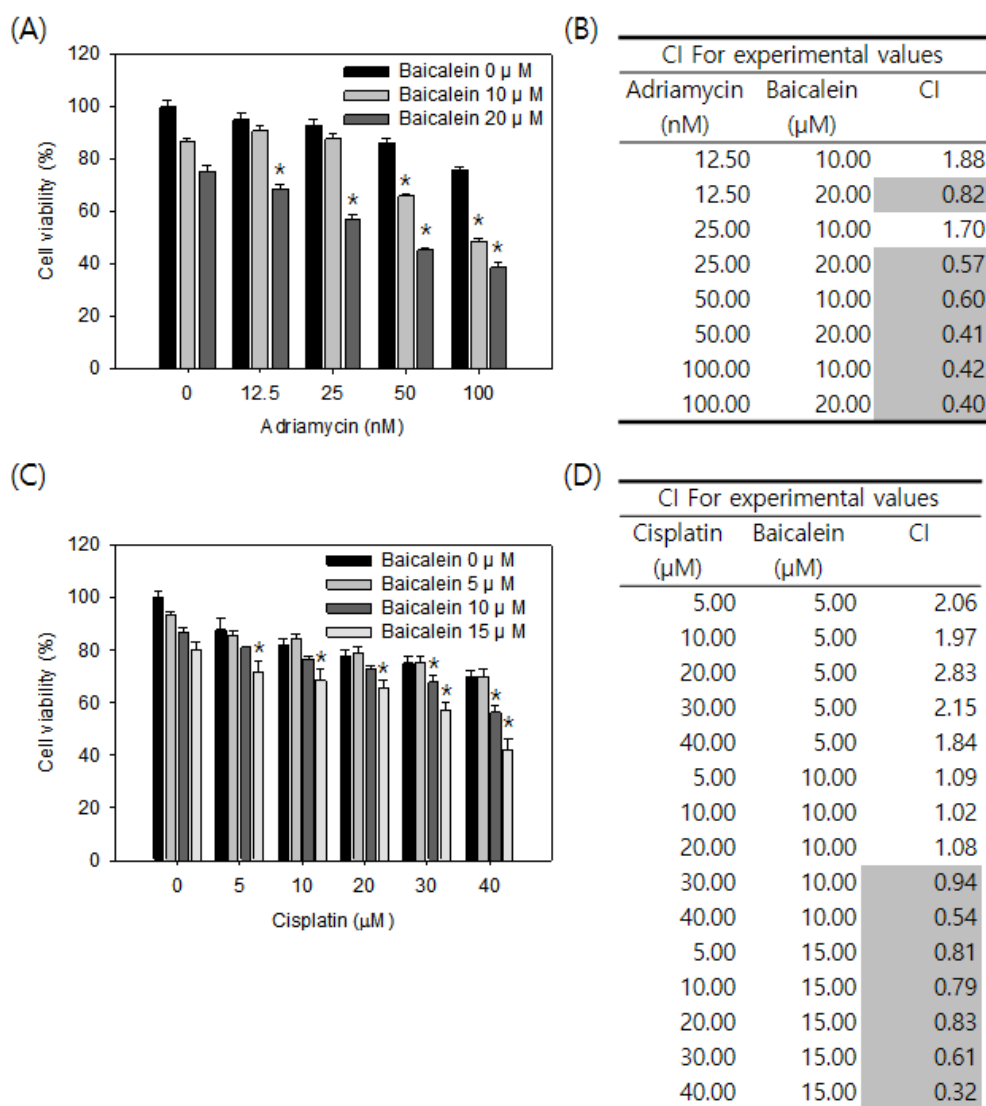


Figure 18. Baicalein co-treatment reversed chemo- resistance in MDA-MB-231/IR cells. Adriamycin (12.5 to 100 nM) was treated on MDA-MB-231/IR with baicalein (10, 20 μM) for 24 h (A). Combination index (CI) value of adriamycin with baicalein was calculated by Calcsyn software (B). Cisplatin (5 to 40 μM) was treated on MDA-MB-231/IR with baicalein (5, 10, 15 μM) for 24 h (C). CI value of cisplatin with baicalein was calculated (D). Values represent means ± standard deviation (SD) (* p < 0.05).

4.20. The expression of IFIT2 affects survival in patients

To figure out the importance of IFIT2, we compared the relationship of the IFIT2 and related genes expression to survival rate of triple negative breast cancer (TNBC) patients by Kaplan-Meier plotter (www.kmplot.com). Using publicly available database, relapse free survival graphs were analyzed by genes expression. To begin with, we performed to create curves that were interpreted as lower IFIT2 expressing patients were related to poor prognosis by lower relapse free survival (RFS), compared to higher expressing TNBC patients (n = 618, Log rank p-value = 0.014, HR = 0.72, probe id: 217502_at; Figure 19A).

We also utilized UCSC Xena (<https://xenabrowser.net/>) and with the cohort of TCGA Breast Cancer from open database, the expression of IFIT2 was decreased in the metastatic type of breast cancer rather than primary tumor or normal tissue (n = 1247, ANOVA One-way, p value = 0.0014, f = 6.593; Figure 19B).

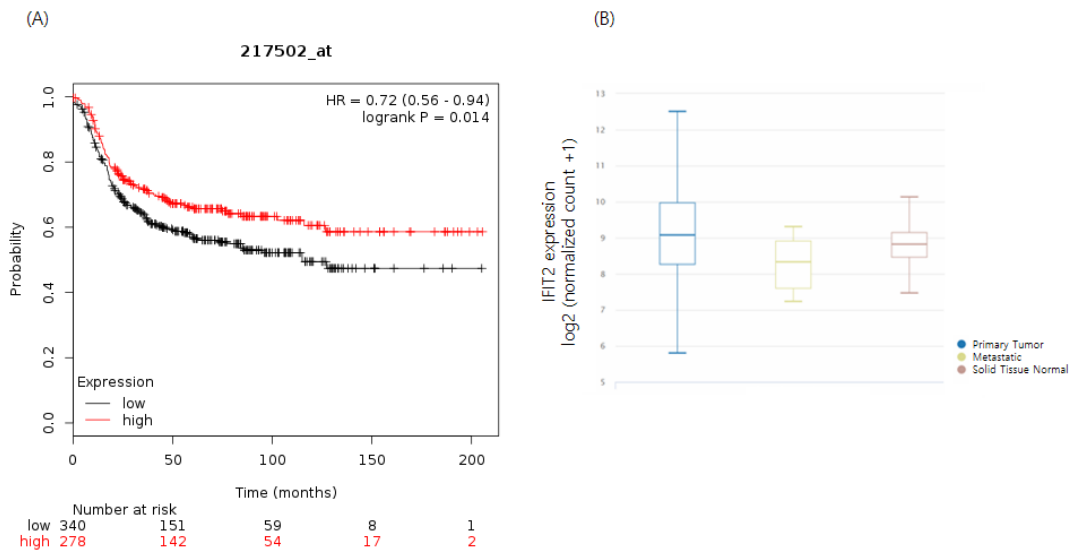


Figure 19. IFIT2 signaling expression is related to poor prognosis in breast cancer. Relapse free survival (RFS) plot of breast cancer analyzed by IFIT2 expression in public database. The expression of IFIT2 is low in metastatic breast cancer compared to normal tissue and primary tumor. The data was analyzed by One-way ANOVA (p value = 0.0014), using breast cancer from the cancer genome atlas (TCGA-BRCA) database.

5. Discussion

Treating breast cancer is still a challenge in spite of the advance in various treatments including surgery, chemotherapy, and radiotherapy. TNBC is a type of breast cancer that characterized by absence of ER, PR, and HER2 which could be target molecules of chemo- or hormone- therapy. Since TNBC is the most malignant subtype with heterogeneous composition of cells, there have been trials to induce TNBC cell death with a treatment of phytochemicals.

Phytochemicals are compounds found in nature, for example, plants or fruits. Flavonoids are one of the subclass of polyphenols of phytochemicals and they are well-known to be beneficent for human health including anti-cancer effect. Flavonols have a hydroxyl group on the 3-position of the C3 ring and previous studies have concluded that the intake of flavonols along with flavones decreased a risk breast cancer (Hui et al., 2013).

We used 10 phytochemicals (3 phenolics, 3 flavones, and 4 flavonols) to test viability on MDA-MB-231/IR. For phenolics, catechol, chlorogenic acid, and protocatechuic acid were used. Apigenin, baicalein, and tangeretin included flavones while kaempferol, myricetin, quercetin, and rutin were belonged to flavonols. Catechol inhibited Stat3/IL-6 signaling pathway and reduced mammosphere formation of breast cancer stem cell derived from MDA-MB-231 (Choi et al., 2018). Chlorogenic acid, along with caffeic acid, partially inhibited the promoter region methylation of RAR β gene on MCF-7 and MDA-MB-231 cells (Lee et al., 2005). Protocatechuic acid treatment lowered the levels of IL-6 and IL-8 and VEGF production on MCF-7 as well as A549, HeLa, and HepG2 cells (Yin et al., 2009). Apigenin targeted TNF α /IL-1 α -induced CCL2 release by inhibiting IKK β - ϵ signaling in MDA-MB-231 breast cancer cells (Bauer et al., 2017). Tangeretin exhibited anti-tumorigenic effects (Lakshmi et al., 2014). Kaempferol induced apoptosis inhibiting ERK activation

under 3D culture environment and conventional 2D condition on breast cancer (Kim et al., 2008). Myricetin induced apoptosis through ERK1/2 and p38 MAPK on breast cancer cells (Knickle et al., 2018). Quercetin down-regulated ALDH1A1, CXCR4, MUC1, and EpCAM and inhibited breast cancer cells (Wang et al., 2018). Baicalein is the main flavone from the roots of *Scutellaria baicalensis* Georgi and is a widely used medicine. We expected that this compound could be one of potential chemicals targeting TNBC cells.

In this study, we found that baicalein shows effects on resistant TNBC cells which we generated from repetitive irradiation, MDA-MB-231/IR. Baicalein reversed not only chemo- and radio- resistance, but also migration, invasion, and stem cell-like properties of the resistant breast cancer cells. While inducing apoptosis on the resistance cells, baicalein also increased the mRNA expression and protein expression of one of cancer resistance genes we identified from transcriptomics analysis of MDA-MB-231/IR cells. The gene is IFIT2 and it has been reported that the expression of IFIT2 induces apoptosis by disturbing mitochondria membrane potential. We confirmed the previous reports of apoptosis induction through conducting Annexin V/PI, JC-1, and cell cycle analysis after treatment of baicalein.

Interferon- induced protein with tetratricopeptide repeats 2 (IFIT2), also called interferon- stimulated gene 54 (ISG54), is one of the four proteins in human characterized by a helix-turn-helix motif (Blatch et al., 1999). IFIT1 and IFIT2 had reported to inhibit mRNA translation and viral mRNA structure by recognizing the lacking O-methylation by interacting with eukaryotic initiation factor 3 (eIF3) (Pichlmair et al., 2011; Zhou et al., 2013). Besides, IFIT2 expression has also been reported to inhibit growth and migration of cancer cells. The increase of IFIT2 expression is reported to happen simultaneously to the induction of apoptosis different stimuli, such as interferon, lncRNAs, miRNAs, and cisplatin, in oral cancer cells, gastric cancer cells, colorectal cancer cells, and osteosarcoma

cells (Jia et al., 2016; Wang et al., 2016; Feng et al., 2014). IFIT2 can also interact with β -tubulin or cytokeratin 18, and regulate cell mitosis or cell motility (Lai et al., 2008; Saha et al., 2006).

Among DEGs which were reported to cancer resistance, only IFIT2 expression was changed after baicalein treatment, which was the most effective phytochemical that we used to kill MDA-MB-231/IR cells. We carried out gene correlation analysis between IFIT2 and genes associated with EMT, stem cell-like character and apoptosis with breast cancer (BRCA) sample in the cancer genome atlas (TCGA). We started with several genes related to migration. Among genes we tested, CXCL10 and VIM were significantly correlated to IFIT2. CXCL10 is chemokine interferon-gamma inducible protein 10 kDa, a member of the CXC chemokine family. CXCL10 is related to inflammation, tumor development, apoptosis and metastasis. The protein is reported to significantly increase apoptotic rate of cancer cells and associated with inhibit migration by regulating JAK2/STAT3 signaling. Vimentin is a structural protein encoded by the VIM gene, and is expressed in mesenchymal cells. This gene is used as a EMT marker during metastatic progression. With 1,075 TCGA-BRCA samples, we performed Pearson analysis and calculated p-value. The results are described on supplementary table 3. The expression of CXCL10 was correlated with IFIT2 (Pearson: 0.3523, P-value: 9.10E-33) while expression of VIM was negatively correlated with the gene (Pearson: -0.0674, P-value: 2.70E-02).

Next, we checked the expression of apoptosis genes with IFIT2. Most of the CASP genes which encode caspases proteins were positively expressed with IFIT2, which confirmed the previous reports that the expression of IFIT2 is associated with apoptosis phenomena (CASP1, CASP5, CASP4, CASP8, CASP7 and CASP3). Also, we performed the analysis with Bcl-2 family proteins, however, only BAK was correlated with IFIT2

within significant p-value.

To sum up, we summarized that IFIT2 is one of the genes of highly annotated pathway of the therapy resistant cell, which is MDA-MB-231/IR, and the expression of IFIT2 was confirmed to be co-expressed with the signaling in breast cancer database from the patients. The expression of IFIT2 is negatively related to cancer migration and invasion whereas it is positively co-expressed with apoptosis signaling in TCGA analysis. Collectively, our data indicated that IFIT2 could be utilized as a prognostic marker in breast cancer.

Upon pathway analysis, to scrutinize the signal that regulates mRNA expression of IFIT2, we utilized opened data from TCGA (the cancer genome atlas, NIH) and compared correlations between IFIT2 and other genes to test if IFIT2 can represent resistance properties of MDA-MB-231/IR. Since it is reported that the mRNA expression of IFIT2 is regulated by JAK/STAT signaling and Wnt/ β -catenin signaling, we tested if the increased IFIT2 expression after baicalein treatment was regulated by JAK/STAT signaling or Wnt/ β -catenin signaling. We performed Pearson correlation analysis between IFIT2 and those signaling molecules on supplementary table 3.

JAK/STAT signaling is one of the signaling that stimulated by IFNs (interferons). The correlation with IFIT2 and STATs were very significantly correlated; STAT1, STAT2, STAT3, STAT4, and STAT5A were positively expressed according to IFIT2. Especially, STAT1 and STAT2 were highly correlated with IFIT2, which confirming previous researches that IFIT2 is transcriptionally regulated with those genes. IFNs stimulate JAKs and STATs and lead to dimer of STATs and go into nucleus for transcription. Meanwhile, IRFs are known to bind to STATs-dimer; for example, IRF9 is known to bind STAT1-STAT2 dimers and form ISGF3 (interferon stimulated gene factor 3) complex to bind to the ISRE (interferon stimulated

response element) promoter to induce ISGs (interferon stimulated genes) which include IFIT2. Since, we also performed comparisons of IRFs with IFIT2. Although IRF9 is well known factor, IRF7, IRF1, IRF2, and IRF5 were also co-expressed with the expression of IFIT2, which supporting that other IRFs can transcript ISRE-containing genes. One of genes that were transcript by STATs is SOCS (suppressor of cytokine signaling, also called CIS; cytokine induced STAT inhibitor) which gives feedback to JAK/STAT signaling. Both SOCS1 and SOCS3 are reported to contain JAK kinase inhibitory region (KIR) and inhibits JAK to phosphorylate STATs. The expressions of SOCS1 and IFIT2 are the downstream genes of STAT1 and STAT2, the two genes were positively correlated. Within the genes belongs to Wnt/ β -catenin signaling, DVL1, DVL2, and DVL3 were correlated to IFIT2 at p-value<0.05. The role of DVLs (the human homolog of the Drosophila gene, dishevelled; Dsh) is inhibiting APC/AXIN/GSK3- β from degradation of β -catenin by Wnt signaling. On TCGA-BRCA (breast cancer) samples, IFIT2 was negatively correlated with DVL1 or DLV2, which means that Wnt/ β -catenin signaling and the expression of IFIT2 were negatively regulated. Once β -catenin is activated, it is reported that it transcripts downstream genes that are often expressed in stem cell. Using Kaplan-Meier plotter, we confirmed IFN/JAK/STAT/IFIT2 signaling in TNBC patients (Supplementary figure 1). The lower expressions of IFNB (Log rank p value = 0.00023, HR = 0.6), JAK1 (Log rank p value = 0.01, HR = 0.65), JAK2 (Log rank p value = 0.0013, HR = 0.66), STAT1 (Log rank p value = 4.2e-10, HR = 0.44), and STAT2 (Log rank p value = 1.2e-05, HR = 0.57) had accompanied with poor prognosis in TNBC patients.

Here we investigated whether baicalein could change the expression of IFIT2 and it reversed the expression of IFIT2 in mRNA level and protein level. Also baicalein treatment

which inversed the IFIT2 expression changed malignant characters of MDA-MB-231/IR cells for example, migration, invasion, and stem cell-like properties. TCGA data analysis revealed that metastatic samples showed lower IFIT2 expressions than primary tumor or normal tissue. KM plots in TNBC patients presented that the patients with low IFIT2 expression level had higher possibility of relapse. In conclusion, baicalein treatment reduced the survival of malignant cancer cells and reverse resistance, migration, invasion, and stem cell-like characteristics of chemo- and radio- resistance cells by increasing IFIT2 expression.

Supplementary table 1. Up-regulated gene list

Difference	Gene name	Difference	Gene name
97.57	AKR1C1	6.18	ERRFI
79.67	FTL	6.03	MOT4
77.43	MK	5.48	IL1B
62.20	LG3BP	4.75	MLH1
46.92	GFPT2	4.07	LIMK1
44.88	NDKB	2.87	NPAS2
44.02	PLSL	2.52	NDST1
42.64	TGFBI	1.93	GMPR2
42.35	AKR1C3	1.78	GGT1
37.77	LAPM5	1.75	OAS3
37.59	CCDC69	1.73	C163B
25.18	CG050	1.67	IL7RA
22.98	PAI2	1.44	NAA25
14.93	RCOR1	1.27	MYH15
14.51	AKR1C2	1.23	TBC16
12.55	TWF1	1.22	LIPB1
8.89	RHG18	1.19	NBAS
7.54	IF16	1.10	FER
6.52	BAG6	0.90	DNLI3

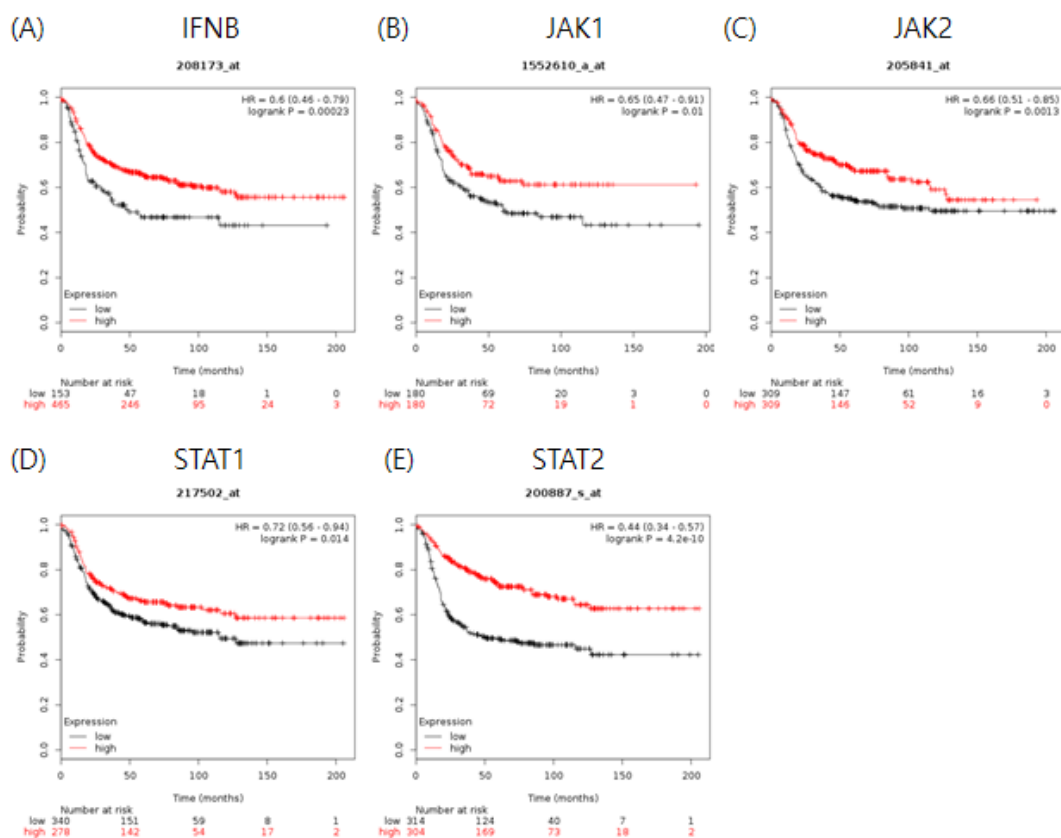
Supplementary table 2. Down-regulated gene list

Difference	Gene name	Difference	Gene name
-0.52	FNIP1	-4.33	PKP3
-1.21	BBX	-4.34	F134A
-1.23	ZBT40	-5.35	2A5E
-1.33	RHG07	-6.38	UBP2L
-1.43	TRAF3	-6.69	ARI2
-1.52	NSD1	-6.69	MEN1
-1.71	PLXA2	-8.91	GLSK
-1.87	TGFA1	-9.733	CD97
-1.95	AGRG6	-10.27	SEN34
-2.06	PDPR	-11.11	TFDP1
-2.22	PHLP1	-13.52	PEG10
-2.29	NAV2	-16.66	ANKH1
-2.41	BUB1	-34.69	SERA
-2.55	RAD21	-69.86	RL21
-2.85	ETS2	-71.11	IFIT3
-3.06	BRD2	-85.89	IFIT2
-3.18	LY65B	-167.432	RS2
-3.51	DAAF5	-210.53	IFIT1
-4.27	SMC4		

Supplementary table 3. Genes expression correlated with IFIT2 signaling pathways predicted by co-expression analysis with TCGA-BRCA dataset.

Signaling	Gene	Pearson	P-value
Migration	CXCL10	0.35	9.1E-33
	VIMENTIN	-0.07	2.7E-02
Apoptosis	CASP1	0.41	2.7E-44
	CASP5	0.23	2.1E-14
	CASP4	0.23	6.2E-14
	CASP8	0.19	7.3E-10
	BAK	0.19	9.3E-10
	CASP7	0.16	8.1E-08
	CASP3	0.09	2.5E-03
JAK/STAT Signaling	STAT1	0.50	6.4E-70
	STAT2	0.45	3.2E-55
	STAT5A	0.23	7.4E-15
	STAT4	0.15	1.1E-06
	SOCS1	0.19	1.4E-10
IRFs	IRF7	0.42	8.4E-47

	IRF9	0.31	5.5E-25
	IRF1	0.23	1.4E-14
	IRF2	0.17	2.5E-08
	IRF5	0.13	3.9E-05
<hr/>			
WNT Signaling	DVL1	-0.07	2.5E-02
	DVL2	-0.09	3.7E-03
<hr/>			



Supplementary figure 1. IFNB/JAK/STAT signaling regulates the expression level of IFIT2, RFS plots of related genes were created by Kaplan-Meier plotter.

6. References

- Al-Hajj et al., 2003, Prospective identification of tumorigenic breast cancer cells
- Amin et al., 2009, Perspectives for Cancer Prevention With Natural Compounds
- Bahmani et al., 2016, Cancer Phytotherapy: Recent Views on the Role of Antioxidant and Angiogenesis Activities
- Bauer et al., 2017, Apigenin inhibits TNF α /IL-1 α -induced CCL2 release through IKK β -epsilon signaling in MDA-MB-231 human breast cancer cells.
- Beachy et al., 2004, Tissue repair and stem cell renewal in carcinogenesis
- Bianchini et al., 2016, Triple-negative breast cancer: challenges and opportunities of a heterogeneous disease
- Bie et al., 2017, Baicalein, a Natural Anti-Cancer Compound, Alters MicroRNA Expression Profiles in Bel-7402 Human Hepatocellular Carcinoma Cells
- Blanco et al., 2002, Correlation of Snail expression with histological grade and lymph node status in breast carcinomas
- Blatch et al., 1999, The tetratricopeptide repeat: a structural motif mediating protein-protein interactions.
- Bockhorn et al., 2013, MicroRNA-30c inhibits human breast tumour chemotherapy resistance by regulating TWF1 and IL-11.
- Buranrat et al., 2015, Cytoprotective effects of ferritin on doxorubicin-induced breast cancer cell death

Carninci et al., 2005, The transcriptional landscape of the mammalian genome

Chang et al., 2003, Gene expression profiling for the prediction of therapeutic response to docetaxel in patients with breast cancer

Chen et al., 2018, Decreased IFIT2 Expression Promotes Gastric Cancer Progression and Predicts Poor Prognosis of the Patients

Choi et al., 2012, Evaluation of the anticancer activities of thioflavanone and thioflavone in human breast cancer cell lines

Choi et al., 2018, Catechol derived from aronia juice through lactic acid bacteria fermentation inhibits breast cancer stem cell formation via modulation Stat3/IL-6 signaling pathway

Cieslik et al., 2017, Cancer transcriptome profiling at the juncture of clinical translation

Conacci-Sorrell et al. 2003, Autoregulation of E-cadherin expression by cadherin-cadherin interactions: the roles of beta-catenin signaling, Slug, and MAPK.

Conacci-Sorrell, M. et al., 2003, Autoregulation of E-cadherin expression by cadherin-cadherin interactions: the roles of β -catenin signalling, Slug, and MAPK

Cragg et al., 2013, Natural products: A continuing source of novel drug leads

Crozier et al., 2009, Dietary phenolics: Chemistry, bioavailability and effects on health

Cui et al., 2017, Inhibition of coiled coil domain containing protein 69 enhances platinum- induced apoptosis in ovarian cancer cells

Dean et al., 2005, Tumour stem cells and drug resistance.

Dent et al., 2007, Triple-negative breast cancer: clinical features and patterns of recurrence

Doherty M.R. et al., 2017, Interferon-beta represses cancer stem cell properties in triple-negative breast cancer

Feng et al., 2014, MicroRNA-645, up-regulated in human adenocarcinoma of gastric esophageal junction, inhibits apoptosis by targeting tumor suppressor IFIT2

Fidler, 2003, The pathogenesis of cancer metastasis: the 'seed and soil' hypothesis revisited.

Friedl, 2011, Cancer Invasion and the Microenvironment: Plasticity and Reciprocity

Haffty et al., 2006, Locoregional relapse and distant metastasis in conservatively managed triple negative early-stage breast cancer

Hemavathy et al., 2000, Snail/Slug family of repressors: slowly going into the fast lane of development and cancer

Huang et al., 2009, Bioinformatics enrichment tools: paths toward the comprehensive functional analysis of large gene lists.

Hui et al., 2013, Flavonoids, Flavonoid Subclasses and Breast Cancer Risk: A Meta-Analysis of Epidemiologic Studies

Hunter N.R. et al., 2013, Mitigation and treatment of radiation-induced thoracic injury with a cyclooxygenase-2 inhibitor, celecoxib

Hughes et al., 2000, Functional discovery via a compendium of expression profiles

Iriti et al., 2017, Rutin, a Quercetin Glycoside, Restores Chemosensitivity in Human

Breast Cancer Cells

Jang et al., 2015, Blockade of Wnt/ β -catenin signaling suppresses breast cancer metastasis by inhibiting CSC-like phenotype.

Jia et al., 2016, The LIM protein AJUBA promotes colorectal cancer cell survival through suppression of JAK1/STAT1/IFIT2 network

Kanadaswami et al., 2005, The antitumor activities of flavonoids

Kim et al., 2008, Sustained ERK activation is involved in the kaempferol-induced apoptosis of breast cancer cells and is more evident under 3-D culture condition

Knickle et al., 2018, Myricetin-induced apoptosis of triple-negative breast cancer cells is mediated by the iron-dependent generation of reactive oxygen species from hydrogen peroxide

Lai et al., 2008, IFN-induced protein with tetratricopeptide repeats 2 inhibits migration activity and increases survival of oral squamous cell carcinoma

Lai et al., 2016, Blocking TNF- α inhibits angiogenesis and growth of IFIT2-depleted metastatic oral squamous cell carcinoma cells.

Lakshmi et al., 2014, Chemotherapeutic effect of tangeretin, a polymethoxylated flavones studied in 7,12-dimethylbenz(α)anthracene induced rat mammary in experimental rats.

Lapidot et al., 1994, A cell initiating human acute myeloid leukaemia after transplantation into SCID mice.

Lee et al., 2005, Inhibition of DNA methylation by caffeic acid and chlorogenic acid, two common catechol-containing coffee polyphenols

Lee et al., 2008, The Role of Ca²⁺ in Baicalein-induced Apoptosis in Human Breast MDA-MB-231 Cancer Cells through Mitochondria- and Caspase-3-dependent Pathway

Lee H.-J. et al., 2013, Combining PARP-1 Inhibition and Radiation in Ewing Sarcoma Results in Lethal DNA Damage

Levin et al., 2008, Estrogen receptors outside the nucleus in breast cancer

Li et al., 2014, AEG-1 Promotes Metastasis Through Downstream AKR1C2 and NF1 in Liver Cancer.

Li et al., 2017, Unraveling the roles of CD44/CD24 and ALDH1 as cancer stem cell markers in tumorigenesis and metastasis

Liu et al., 2013, CD133⁺ cells with cancer stem cell characteristics associates with vasculogenic mimicry in triple-negative breast cancer

Liu et al., 2015, Intracrine Androgens and AKR1C3 Activation Confer Resistance to Enzalutamide in Prostate Cancer

Liu T. J. et al., 2013, CD133⁺ cells with cancer stem cell characteristics associates with vasculogenic mimicry in triple-negative breast cancer

Lu et al., 2009, Breast Cancer Metastasis: Challenges and Opportunities

Luzhna et al., 2015, Altered radiation responses of breast cancer cells resistant to hormonal therapy

Ma et al., 2008, Extracellular matrix protein β ig-h3/TGFBI promotes metastasis of

colon cancer by enhancing cell extravasation

Ma et al., 2016, Baicalein suppresses metastasis of breast cancer cells by inhibiting EMT via downregulation of SATB1 and Wnt/ β -catenin pathway

Meacham et al., 2013, Tumor heterogeneity and cancer cell plasticity

Mocanu et al., 2015, Chemoprevention of breast cancer by dietary polyphenols

Nowak et al., 2013, Plant Polyphenols as Chemopreventive Agents

Oakman et al., 2010, Management of triple negative breast cancer

Ohsugi et al., 2017, Decreased expression of interferon-induced protein 2 (IFIT2) by Wnt/ β -catenin signaling confers anti-apoptotic properties to colorectal cancer cells.

Oracz et al., 2015, The Content of Polyphenolic Compounds in Cocoa Beans (*Theobroma cacao* L.), Depending on Variety, Growing Region, and Processing Operations: A Review

Pichlmair et al., 2011, IFIT1 is an antiviral protein that recognizes 5'-triphosphate RNA.

Ravishankar et al., 2013, Flavonoids as prospective compounds for anti-cancer therapy

Rodgers et al., 1998, The effect of the flavonoids, quercetin, myricetin and epicatechin on the growth and enzyme activities of MCF7 human breast cancer cells

Saha et al., 2006, Identification of Japanese encephalitis virus-inducible genes in mouse brain and characterization of GARG39/IFIT2 as a microtubule-associated protein.

Scharenberg C. W. et al., 2002, The ABCG2 transporter is an efficient Hoechst 33342 efflux pump and is preferentially expressed by immature human hematopoietic

progenitors

Schatton et al., 2009, Identification and targeting of cancer stem cells.

Siegel et al., 2016, Cancer statistics, 2016

Simpson et al., 2012, An in vitro investigation of metabolically sensitive biomarkers in breast cancer progression

Staunton et al., 2001, Chemosensitivity prediction by transcriptional profiling

Stawowczyk et al., 2011, The interferon stimulated gene 54 promotes apoptosis

Sun et al., 2017, Midkine promotes hepatocellular carcinoma metastasis by elevating anoikis resistance of circulating tumor cells

Takahashi et al., 2012, Up-regulation of plakophilin-2 and Down-regulation of plakophilin-3 are correlated with invasiveness in bladder cancer

Thiery, J. P., 2003, Epithelial–mesenchymal transitions in development and pathologies

Velculescu et al., 1997; Characterization of the yeast transcriptome

Wang et al., 2010, Flavonoid baicalein suppresses adhesion, migration and invasion of MDA-MB-231 human breast cancer cells

Wang et al., 2015, Baicalein attenuates renal fibrosis by inhibiting inflammation via down-regulating NF- κ B and MAPK signal pathways

Wang et al., 2016, Long non-coding RNA LINC00161 sensitises osteosarcoma cells to cisplatin-induced apoptosis by regulating the miR-645-IFIT2 axis

Wang et al., 2018, Quercetin Inhibits Breast Cancer Stem Cells via Downregulation of Aldehyde Dehydrogenase 1A1 (ALDH1A1), Chemokine Receptor Type 4 (CXCR4), Mucin 1 (MUC1), and Epithelial Cell Adhesion Molecule (EpCAM)

White et al., 2015, Galectin-3 Binding Protein Secreted by Breast Cancer Cells Inhibits Monocyte-Derived Fibrocyte Differentiation.

Wu et al., 2011, Baicalein mediates inhibition of migration and invasiveness of skin carcinoma through Ezrin in A431 cells

Yang et al., 2018, Molecular identification and transcriptional regulation of porcine IFIT2 gene

Yin et al., 2009, Apoptotic Effects of Protocatechuic Acid in Human Breast, Lung, Liver, Cervix, and Prostate Cancer Cells: Potential Mechanisms of Action

Zhou et al., 2009, Tumour-initiating cells: challenges and opportunities for anticancer drug discovery.

Zhou et al., 2013, Interferon induced IFIT family genes in host antiviral defense.

Zhu et al., 2018, AKR1C1 Activates STAT3 to Promote the Metastasis of Non-Small Cell Lung Cancer.

